REGULAR ARTICLE

A theoretical study of the thermodynamics and kinetics of small organosulfur compounds

Aäron G. Vandeputte · Marie-Françoise Reyniers ·
Guy B. Marin

Abstract The performance of a large set of ab initio procedures in predicting geometries, thermochemical and kinetic data of small sulfur compounds is assessed. Geometries and thermochemical data for H_2S, $(CH_3)_2S$, H_2S_2, $(CH_3)_2S_2$ and $H_2C=S$ are studied using the HF method, density functional theory methods (B3LYP, BHandHLYP, MPW1PW91 and BMK), post-HF methods [MP2, MP3, MP4, CCSD, CCSD(T) and QCISD] and composite techniques (G3, G3B3, CBS-QB3 and W1U). A set of five reactions involving these small organosulfur compounds is studied and the influence of the level of theory on transition state geometries, reaction barriers and rate coefficients is assessed. Independent of the level of theory used, accurate geometries are obtained with the 6-311G(2d,d,p) and cc-pVTZ basis sets, both reproducing experimental bond lengths and bond angles within 2 pm and 0.5°. Besides composite methods, the BMK/cc-pVTZ method is the only studied method that succeeds to predict standard enthalpies of formation within 10 kJ mol^{-1} of the experimental data. The best agreement with experimental rate coefficients is obtained with the BHandHLYP/cc-pVTZ method, closely followed by the composite methods and the BMK/cc-pVTZ method. All these methods succeed to reproduce the experimental rate coefficients within a factor 4. To obtain an accurate prediction of both thermochemical and kinetic data for organosulfur compounds, the commonly used composite methods G3B3 and CBS-QB3 and the BMK/cc-pVTZ method prove to be valuable tools.

Keywords Ab initio methods ·
Organosulfur compounds · Thermochemistry ·
Reaction kinetics

Abbreviations
BDE   Bond dissociation enthalpy
DFT   Density functional theory
HF   Hartree Fock
HO   Harmonic oscillator
MAD   Mean absolute deviation
RAFT   Reversible addition–fragmentation chain transfer

List of symbols
E Energy (J)
h Planck's constant (6.62×10^{-34} J s)
k Rate coefficient (m^{3}mol^{-1} s^{-1})
k_b Boltzmann constant (1.38×10^{-23} J K^{-1})
n Number of single events
q Molar partition function
R Universal gas constant (8.314510) (J mol^{-1} K^{-1})
S Entropy (J mol^{-1} K^{-1})
T Temperature (K)

Greek symbols
v Frequency (cm^{-1})
ρ Relative deviation k_{max}/k_{min} between experimental and ab initio calculated rate coefficients

Subscript
atom   Atomic
arithm   Arithmetic
cal   Calculated
exp   Experiment(al)

A. G. Vandeputte · M.-F. Reyniers (✉) · G. B. Marin
Laboratory for Chemical Technology, Faculty of Engineering, Ghent University, Krijgslaan 281 S5, 9000 Ghent, Belgium
e-mail: Mariefrancoise.Reyniers@Ugent.be

f   Formation
geom   Geometric
opt   Optical isomers
r/reac   Reaction
tot   Total
‡   Corresponding to the transition state excluding
           the motion along the reaction coordinate

Superscript
°   Standard state (1 bar)
‡   Corresponding to the transition state

1 Introduction

Sulfur is one of the most abundant elements on earth and is an essential component of all living cells. Atmospheric sulfur compounds mainly result from burning of fossil fuels and in smaller amounts from the action of anaerobic bacteria and volcanic activity. Reactions of these sulfur compounds with other atmospheric species can lead to the formation of sulfuric acid and hence contribute to acid rain. Large efforts are therefore made to understand the complex atmospheric chemistry involving these sulfur compounds [1] and desulfurization processes are developed to produce cleaner fuels with less sulfur content [2–4]. A wide variety of organosulfur compounds are applied in current industrial processes. Alkylsulfides and their derivates, for example, are used as coke and CO inhibiting additives during the steam cracking of crude oil fractions to olefins [5, 6]. In free radical polymerization, sulfur compounds are frequently used to control the molecular mass of the polymer [7]. Other applications range from the production of pharmaceuticals and antioxidants up to the degradation of insecticides [8, 9]. To optimize the deployment of sulfur compounds during chemical processes an accurate reaction network is required that succeeds in describing the specific reaction behaviour of these compounds under the process conditions. In the case of radical chemistry, reaction networks can easily contain up to thousands of elementary reactions for which accurate thermodynamic and kinetic parameters need to be at hand.

Despite their industrial relevance, experimental data about the thermochemistry and kinetics of organosulfur compounds are rather scarce. As scientists become more aware about the useful reaction behaviour of some of these compounds and about the major role they play in everyday biological processes, the interest in sulfur chemistry has firmly grown the last decades. Benson [10] was one of the first authors to provide a comprehensive survey of the experimental data acquired up to 1978 and also formulated group additive contributions for the prediction of thermodynamic properties of sulfur containing molecules. Reliable

thermodynamic data are hard to obtain mostly due to the high instability of the gaseous sulfur compounds. Older data are therefore often revised and subjected to significant changes [11]. Most experimental studies aiming at the determination of accurate rate coefficients for elementary reactions involving organosulfur compounds were carried out in the late seventies and eighties. Among these, radical substitution reactions of hydrogen atoms with dimethylsulfide [12], dimethyldisulfide [13] and diethyldisulfide [14], and hydrogen abstraction reactions between (a) hydrogen and dimethylsulfide [15], (b) hydrogen and hydrogensulfide [16] and (c) methyl and thiols [17] are well documented.

With the increasing computer capacity ab initio methods are nowadays extensively employed for the calculation of thermodynamic properties. Benchmark studies testing the reliability of theoretical data against experimental data indicate that complete basis set techniques such as CBS-Q [18] and G3 [19] are highly suitable for acquiring thermochemical data for sulfur compounds [20, 21]. Also S–H bond dissociation enthalpies (BDEs) have already been extensively studied. Fu et al. [22] reported BDE(S–H) values of para and meta substituted thiophenols at the UB3LYP/6-311++G(d,p) level of theory. Better agreement with experiment was found by Chandra et al. [23] using the (RO)B3LYP formalism introduced by Wrigth et al. [24]. Do Couto et al. [25] studied the influence of the level of theory on theoretical S–H BDEs and emphasised the importance of an appropriate complete basis set to obtain accurate BDEs.

Recent advances in computational chemistry and the development of improved theoretical methods make it also possible to accurately study the reaction behaviour of small organosulfur compounds. Due to their relevance for polymer chemistry, the addition reactions of $C^{\bullet}H_3$ [26, 27] and $H^{\bullet}$ [28] to C=S double bonds are among those theoretically studied reactions. Coote et al. [26] concluded that DFT methods are not suitable to study the methyl addition reactions to C=S double bonds, while HF methods fail to give proper transition state structures for methyl shifts in $CH_3CH_2S^{\bullet}$, the addition product of $C^{\bullet}H_3$ and $H_2C=S$. In more recent work of Izgorodina and Coote [29] an extensive study was conducted towards addition–fragmentation reactions on C=S double bonds in the frame of reversible addition–fragmentation chain transfer (RAFT) polymerization. The authors propose using a three layer ONIOM method to study the reaction mechanism. Benassi [30] studied the oxidation of CH_3SH to CH_3SSCH_3 by comparison of kinetic parameters calculated on the MP2(full)/6-31G* level of theory with data calculated using composite methods. Variational transition state rate coefficients for the H abstraction of H_2S by $C^{\bullet}H_3$ and $O^{\bullet}H$ are reported by Mousavipour et al. [31].

Also isomerisation reactions of small organosulfur compounds have been the subject of detailed studies. Pei et al. [32] studied the tautomerization reaction of $CH_3S \leftrightarrow CH_2SH$ with HF/B3LYP/MP2, while Chui et al. [33] used the Gaussian complete basis set methods to study the different isomers of $C_2H_3S^+$, C_2H_5S [34] and C_3H_6S [35]. The latter authors also reported energy profiles of dissociation channels for some of the studied unstable isomers and found good agreement with mass spectroscopic results. Also worth mentioning is the theoretical study of Gomez et al. [36] in which the Claisen rearrangement of allyl aryl thio ethers is discussed.

A lot of research towards the accurate prediction of barrier heights is conducted by the research group of Truhlar et al. [37–39]. Recently, Zheng et al. [40] extensively studied the barrier height predicting abilities of 205 methods. These authors found that DFT methods such as BB1K, PWB6K and BMK are powerful tools to predict barrier heights. These methods scale with N^4 and perform similarly as the most accurate N^5 methods. Of all studied methods, the G3SX method succeeds to yield most accurate energy barriers, closely followed by CCSD(T)/aug-cc-pVTZ. The reaction set studied by Zheng et al. [40] contains only one reaction involving a third row atom, i.e. the H abstraction by H from H_2S. Barrier heights for four additional reactions involving small organosulfur compounds will be studied in this work. Besides barrier heights, classical transition state rate coefficients will be assessed and compared with experimental data if available.

In the present work the accuracy of several low and high level of theory methods to reproduce experimental thermochemical and kinetic data for small organosulfur compounds is evaluated. The aim is to pinpoint cost efficient methods that can be used for further studies of the chemistry of sulfur compounds. Calculations were performed with the HF method, six post-HF methods (MP2, MP3, MP4, CCSD, CCSD(T) and QCISD), four popular DFT methods (B3LYP, MPW1PW91, BHandHLYP and BMK) and four composite methods (G3, G3B3, CBS-QB3 and W1U). In this work, geometry optimizations and energy calculations are performed on dihydrogensulfide (H_2S), dimethylsulfide [$(CH_3)_2S$], dihydrogendisulfide (H_2S_2), dimethyldisulfide [$(CH_3)_2S_2$] and thioformaldehyde ($H_2C=S$). The different levels of theory are evaluated using seven different basis sets: 6-31G, 6-31++G, 6-311G, 6-311++G, 6-311G(2d,d,p), cc-pVDZ and cc-pVTZ. Transition state theory is used to calculate rate coefficients for five reactions involving small sulfur compounds: (a)–(b) the H abstraction reactions from H_2S by the hydrogen and methyl radical, (c)–(d) the homolytic substitution reactions of $H^\bullet$ on dimethylsulfide and dimethyldisulfide, and (e) the addition of methyl on thioformaldehyde with the formation

of an ethylthiyl radical. In Sect. 3 of this work, the computational methods used in this study are briefly presented and the calculation of the standard enthalpies of formation, standard entropies and rate coefficients from theoretical data is discussed. Next, the results of an extended level of theory study are presented. The performance of the various methods is evaluated by comparison with experimental data and the feasibility of using one or more levels of theory to accurately compute thermochemical data and rate coefficients for organosulfur compounds is assessed.

2 Computational methods

2.1 Thermodynamic properties

All calculations were performed using the *Gaussian 03* computational package [41]. Transition states were located using the *opt(calcfc,ts)* option. If no analytic force constants were available for the method, initial force constants were estimated (using the *NewEstFC* command) or B3LYP force constants were provided as initial guess. A large set of ab initio methods are investigated ranging from the most simple HF method [42] to advanced composite techniques such as the Gaussian-3 theory [19, 43], the CBS-QB3 complete basis set method [44] and the Weiszmann-1 method [45]. As these composite methods can be computationally very demanding, attention will also be paid to the computationally less intensive basis set extrapolation procedure developed by Truhlar [46]. Fast et al. [47] have shown that a simple two parameters extrapolation scheme for MP2/cc-pVDZ and MP2/cc-pVTZ energies (MP2/∞), succeeds to yield atomization energies for small compounds within 8 kJ mol^{-1} of accuracy. Perturbative methods can be susceptible for mixing of their ground state with higher spin states [48]. If this is the case, more accurate data can then be obtained by spin-projected projected methods [49]. The spin projected MP2 energies presented in this work were obtained from calculations on the MP2 optimized geometries (PMP2//MP2).

Standard enthalpies of formation at 298 K, $\Delta_f H^o$ (298 K), are obtained by subtracting the calculated atomization enthalpy of the sulfur compound, $\Delta_{atom} H^o_{cal}$ (298 K), from the experimental atomization enthalpies of its constituent elements, $\Delta_{atom} H^o_{exp}$ (298 K):

$$\Delta_f H^o(S_m C_n H_o; 298\,K) = \left[m\Delta_{atom} H^o_{exp}(S; 298\,K) \right.$$
$$+ n\Delta_{atom} H^o_{exp}(C; 298\,K) + o\Delta_{atom} H^o_{exp}(H; 298\,K) \right]$$
$$- \Delta_{atom} H^o_{cal}(S_m C_n H_o; 298\,K) \tag{1}$$

with

$$\Delta_{\mathrm{atom}}H^{\mathrm{o}}_{\mathrm{cal}}(\mathrm{S}_m\mathrm{C}_n\mathrm{H}_o; 298\,\mathrm{K}) = \big[mH^{\mathrm{o}}_{\mathrm{cal}}(\mathrm{S}; 298\,\mathrm{K})$$
$$+ nH^{\mathrm{o}}_{\mathrm{cal}}(\mathrm{C}; 298\,\mathrm{K}) + oH^{\mathrm{o}}_{\mathrm{cal}}(\mathrm{H}; 298\,\mathrm{K})\big]$$
$$- H^{\mathrm{o}}_{\mathrm{cal}}(\mathrm{S}_m\mathrm{C}_n\mathrm{H}_o; 298\,\mathrm{K}) \tag{2}$$

$\Delta_{\mathrm{atom}}H^{\mathrm{o}}_{\mathrm{exp}}$ (298 K) is sometimes referred to as the atomic enthalpy of formation. The following experimental enthalpies were used: $\Delta_{\mathrm{atom}}H^{\mathrm{o}}_{\mathrm{exp}}$ (S; 298 K) = 276.98 kJ mol^{-1}, $\Delta_{\mathrm{atom}}H^{\mathrm{o}}_{\mathrm{exp}}$ (C; 298 K) = 716.68 kJ mol^{-1} and $\Delta_{\mathrm{atom}}H^{\mathrm{o}}_{\mathrm{exp}}$ (H; 298 K) = 217.998 kJ mol^{-1} [11]. To improve the accuracy of ab initio methods in predicting standard enthalpies of formation, extra correction factors are often added to Eq. 1 accounting for the error made per atom [50]. As in this work the number of atoms in the considered compounds is restricted to maximum 11 atoms, no corrections were applied.

The standard molar entropy S^{o} is obtained from the *Gaussian* output and is calculated from the total partition function, q_{tot}, according to Eq. 3:

$$S^{\circ} = R\left(\ln q_{\mathrm{tot}} + T\frac{\partial \ln q_{\mathrm{tot}}}{\partial T} + \ln n_{\mathrm{opt}}\right) \tag{3}$$

The total partition function q_{tot} is a measure for the energetic degrees of freedom of a molecule and is composed of contributions originating from electronic and nuclear motions. If all modes are separable the total partition function can be written as a product of four contributions, i.e. (a) the electronic partition function, (b) the translational partition function evaluated at 1 atm, (c) the rotational partition function and (d) the vibrational partition function. The electronic partition function equals 1 for singlets and 2 for radicals. A correction n_{opt} enters Eq. 3 to account for the number of optical isomers. As each optical isomer represents a distinct but energetically equivalent state it must be included in the calculation of the total partition function [51]. Contrary to the number of optical isomers, external and internal symmetry numbers are implicitly taken into account within the *Gaussian* partition functions.

Scott and Radom [52] determined scaling factors for zero point vibrational energies for HF, post-HF and DFT methods. In analogy with their results we opted to apply a scaling factor of 0.92 for HF, 0.97 for post-HF methods and 0.99 for DFT methods, independent of the basis set used. The default scaling factors of 0.8929, 0.96, 0.99 and 0.985 were used for respectively G3, G3B3, CBS-QB3 and W1U.

2.2 Rate coefficients

Rate coefficients k are calculated using the conventional transition state theory in the high pressure limit. This implies that for bimolecular reactions k is calculated according to Eq. 4 [53]:

$$k(T) = n_e \kappa(T) \frac{k_B T}{h} \frac{q_{\ddagger}}{q_A q_B} e^{-\frac{\Delta^{\ddagger}E}{RT}} \tag{4}$$

with $\Delta^{\ddagger}E$ the zero point corrected electronic activation barrier and q_A, q_B, $q_{\ddagger}$ the total molar partition functions per unit volume of respectively the reactants (A and B) and the transition state. In Eq. 4 quantum mechanical tunnelling effects are accounted for by the transmission coefficient $\kappa(T)$. Imai et al. [54] showed that tunneling contributions can have a significant contribution to the rate coefficients for hydrogen abstraction reactions from organosulfur compounds. The authors reported experimental rate coefficients for the reactions $H_2S + CH_3 \rightarrow SH + CH_4$ and $D_2S + CH_3 \rightarrow SD + CH_3S$ and showed that the rate coefficients of both reactions differ by a factor 2.2 at 573 K up to a factor 2.7 at 473 K. In this work the transmission coefficient is calculated according to the Eckart procedure [55]. This procedure has shown to be a reliable and cost-effective method to quantify the contribution of quantum mechanical effects on rate coefficients [56, 57]. n_e in Eq. 4 accounts for chirality in the transition state or in the reactants [51].

As a measure for the deviation between experimental and ab initio rate coefficients, a factor ρ is defined according to Eq. 5:

$$\rho = \begin{cases} \frac{k_{\mathrm{calc}}}{k_{\mathrm{exp}}} & k_{\mathrm{calc}} > k_{\mathrm{exp}} \\ \frac{k_{\mathrm{exp}}}{k_{\mathrm{calc}}} & k_{\mathrm{exp}} > k_{\mathrm{calc}} \end{cases} \tag{5}$$

The factor ρ is a value larger than 1 and is a measure for the relative deviation between two rate coefficients. For a set of reactions, $\langle\rho\rangle$ can be calculated as the arithmetic or geometric average value:

$$\langle\rho\rangle_{\mathrm{arithm}} = \sum_i^{n_{\mathrm{reac}}} \frac{1}{n_{\mathrm{reac}}}\rho_i, \quad \langle\rho\rangle_{\mathrm{geom}} = \sqrt[n_{\mathrm{reac}}]{\prod_i^{n_{\mathrm{reac}}} \rho_i} \tag{6}$$

with n_{reac} the number of reactions considered in the set and ρ_i equal to the factor ρ for reaction i. In general, $\langle\rho\rangle_{\mathrm{arithm}}$ pictures the agreement between the calculated and experimental rate coefficients quite well. However, when the ρ_i values differ with some orders of magnitude, the arithmetic mean approaches to $\rho_{\mathrm{max}}/n_{\mathrm{reac}}$. For this reason, $\langle\rho\rangle_{\mathrm{geom}}$ values are also reported in this work.

3 Results and discussion

3.1 Geometry

A small set of geometrical data was gathered from the NIST Computational Chemistry Comparison and Benchmark
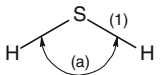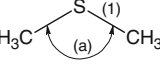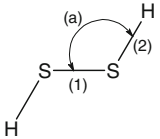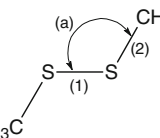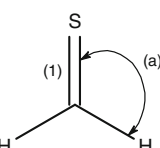
Database [58]. The set of experimental data contains five small organosulfur compounds, as can be seen from Table 1. Both S–H, S–C, S–S and S=C bond lengths as well as H–S–H, C–S–C, S–S–H, S–S–C and H–C=S bond angles can be identified within these compounds. The influence of polarization functions and diffuse functions on the geometry was assessed. While adding polarization functions give more bonding flexibility to the orbitals, addition of diffuse functions permits a more accurate description of the fading tail of the orbitals distant from the nuclei. Several literature reports indicate that polarization functions are indispensible for the calculation of accurate geometries and energies for sulfur compounds [59, 60] and for studying the energy barriers of reactions involving hetero-elements [61].

Geometry optimizations were performed on all the levels of theory under study and this for five Pople type basis sets, i.e. 6-31G, 6-31++G, 6-311G, 6-311G(2d,d,p) and 6-311++G(2d,p), and two Dunning correlation consistent basis sets, i.e. cc-pVDZ and cc-pVTZ. Montgomery

et al. [44] have shown that for B3LYP the 6-311G(2d,d,p) basis set yields accurate geometries and is the smallest basis set able to attain the full potential of the method to calculate frequencies. Dunning consistent basis sets have the advantage to provide a consistent set of basis sets for extrapolating to the basis set limit but can be computational more expensive as they use large sets of polarization functions [62, 63]. Martin and Uzan [64] showed that the basis set convergence could even be accelerated when a single high-exponent d function is added to the cc-pVnZ basis set, leading to revised correlation consistent basis sets for the elements Al to Ar [65].

Mean absolute deviations between the calculated and experimental bond lengths and bond angles are plotted respectively in Figs. 1 and 2. Detailed results of this study can be found in Tables S-1 and S-2 of the supporting information. Figure 1 illustrates that all different levels of theory tend to yield equally accurate data when the same basis set is used. For smaller basis sets, the results obtained with HF and most DFT methods are in slightly better

Table 1 Set of experimental bond lengths, bond angles, $\Delta_f H^o$s and S^os [68]

Molecule	Bond length (pm)	Bond angle (°)	$\Delta_f H^o$ (298 K) (kJ mol^{-1})	S^o (298 K) (J mol^{-1} K^{-1})
	(1) 132.8	(a) 92.2	-20.6 ± 0.5 [89]	205.81 ± 0.05 [89]
	(1) 180.2	(a) 98.9	-37.5 ± 2.0 [90]	285.96* [91]
	(1) 205.6 (2) 134.2	(a) 97.9	15.5* [91]	252.4* [91]
	(1) 203.8 (2) 181.0	(a) 102.8	-24.1 ± 2.3 [90]	336.8* [91]
	(1) 161.1	(a) 121.7	114.7 ± 8.4 [73] 86.7 ± 8.0 [69]	234.4 ± 4 [10]

* No accuracy available

agreement with experiment than those obtained with the post-HF methods. For example, with a 6-31G basis set, the MADs on the bond lengths for HF and the DFT methods vary around 9 pm (with exception of the BMK functional), while all post-HF methods yield MADs ranging between 11 and 13 pm. When non-polarized basis sets are used, the bond lengths are overestimated. For example with the 6-31G basis set, the ab initio S–H, S–C and S–S bond
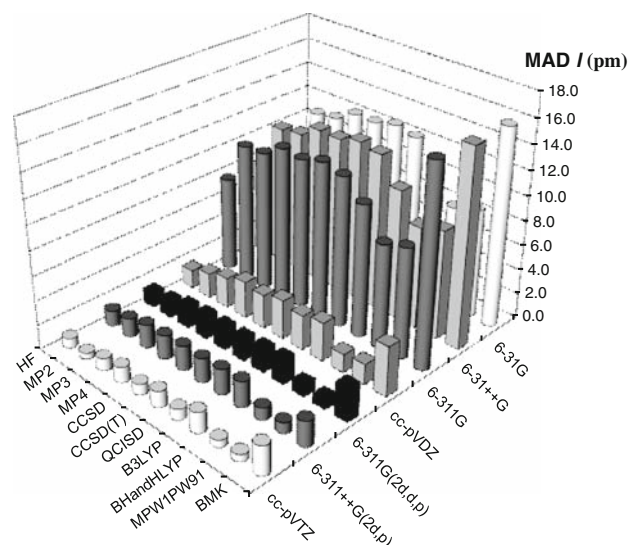
Fig. 1 Influence of the level of theory and basis set on the mean absolute deviation (MAD) between the ab initio and experimental bond lengths for the five compounds presented in Table 1
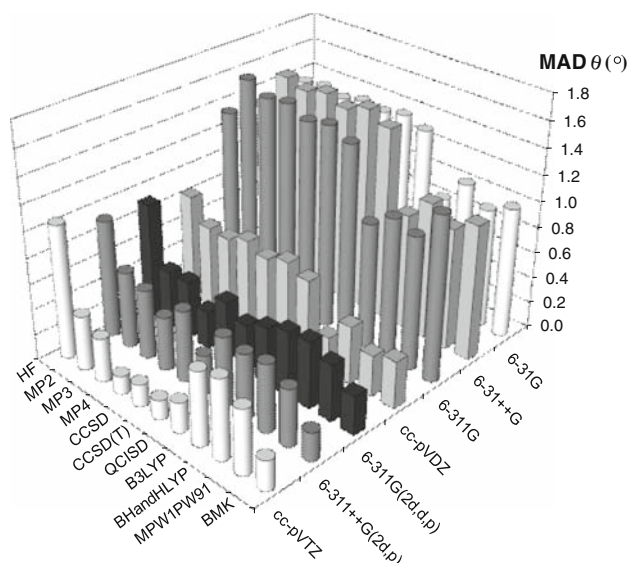
Fig. 2 Influence of the level of theory and basis set on the mean absolute deviation (MAD) between the ab initio and experimental bond angles for the five compounds presented in Table 1

lengths are respectively 5, 10 and 20 pm longer than the experimental values. This is in agreement with the findings of Altmann et al. [59]. No significant better agreement with experiment is obtained with a 6-311G basis set compared to its double zeta basis set analogue, 6-31G. As similar results are obtained with 6-31G and 6-31++G, it is concluded that addition of diffuse functions has little effect on the geometry. In contrast, addition of polarization functions significantly increases the agreement with the experimental bond lengths: the MADs on the bond lengths generally decrease from 10 pm obtained with the non-polarized basis sets to approximately 2 pm obtained with the polarized basis sets. As expected, basis sets with larger sets of polarization functions reproduce the experimental data more accurately: with the cc-pVTZ basis set more accurate bond lengths are obtained compared to 6-311G++(2d,p), which in its turn outperforms the cc-pVDZ basis set. The similar results obtained with 6-311G++(2d,p) and 6-311G(2d,d,p) indicate that both the addition of 2d polarization functions to C atoms and diffuse functions has only a minor effect on the calculated geometries of the studied organosulfur compounds. With the 6-311G++(2d,p) basis set, accuracies up to 1 pm can be obtained when using DFT methods while with the cc-pVTZ basis set accuracies up to 0.5 pm can be reached with the post-HF methods. The better performance of cc-pVTZ is mainly due to a better description of the S–S bond lengths. When DFT methods are used, the S–S bond lengths are predicted 1 pm more accurate with cc-pVTZ compared to 6-311G++(2d,p) while for the HF based methods this improvement can amount up to 3 pm.

From Fig. 2 it is seen that analogous conclusions can be drawn for bond angles as for bond lengths: (1) when the basis set does not contain polarization functions, similar results are obtained with the 6-31G and 6-311G basis sets irrespective of the use of diffuse functions and (2) inclusion of polarization functions significantly increases the agreement with the experimental bond angles. With the 6-31G, 6-31++G and 6-311G basis sets, the mean absolute deviation between the experimental and calculated bond angles fluctuates around 1.1°. Inclusion of polarization functions lowers the MADs to approximately 0.5° independent of the level of theory used. For the HF based methods, most accurate bond angles are obtained with the cc-pVTZ basis set, while for the DFT methods more accurate bond angles are obtained with the cc-pVDZ basis set. Polarization functions tend to have less influence on the results of DFT methods than on the HF based methods.

It is concluded that for the accurate prediction of geometries, polarization functions are indispensable. The study shows that an extension of the basis set with 2d, d and p polarization functions for respectively S, C and H

already suffices to predict the bond lengths and bond angles of organosulfur compounds within 2 pm and 0.5° accurate, independent of the level of theory used. Geometry optimizations performed on the CCSD(T)/6-311G(3df,2dp) level of theory for H_2S and $H_2C=S$ show no further increase of the accuracy compared with the cc-pVTZ basis set (see Fig. S-1 of the supporting information). DFT methods tend be less susceptible for the number of polarization functions in the basis set: similar accuracies are obtained for 6-311G(2d,d,p) and cc-pVTZ. For the HF based methods it is observed that the cc-pVTZ basis set performs slightly better than 6-311G(2d,d,p), mainly caused by a better prediction of the S–S bond lengths. Our results are in agreement with the data presented by Altmann et al. [66, 67] who also examined the performance of HF, B3LYP and MP2 in predicting geometries for a set of approximately 20 sulfur compounds. The authors reported that for a cc-pVTZ basis set all three methods yield similar accuracies, predicting the bond lengths within 1 to 2 pm and bond angles within 2° accurate.

3.2 Thermochemistry

Besides geometries, the accuracy in predicting standard entropies and standard enthalpies of formation was assessed for a wide variety of levels of theory and basis sets. The experimental set of S^os and $\Delta_f H^o$s used for this study can be found in Table 1. For thioformaldehyde, the NIST chemistry webbook [68] provides two experimental values which differ with 28 kJ mol^{-1}. The value reported by Roy and McMahon [69], 86.7 ± 8.0 kJ/mol at 298 K, was calculated from the experimentally determined proton affinity for thioformaldehyde. Based on a proton affinity of 757 ± 4 kJ mol^{-1}, $\Delta_f H^o$ (0 K) (CH$_2$SH$^+$) = 870 ± 4 kJ mol^{-1} and the enthalpy of the proton of 1,536 kJ mol^{-1} [69], these authors found $\Delta_f H^o$ (0 K) of $H_2C=S$ to amount to 90.5 kJ mol^{-1}. This value was supported by the findings of Jones and Lossing [70] who had previously argued that the heat of formation of thioformaldehyde should be lower than 100 ± 10 kJ mol^{-1}. More recently, Ruscic and Berkowitz [71] reassessed $\Delta_f H^o$ (0 K) (CH$_2$SH$^+$) and found a value of 885 ± 8 kJ mol^{-1}. Taking into account the $\Delta_f H^o$ (0 K) (CH$_2$SH$^+$) determined by Ruscic and Berkowitz [71] and the more recently reported $\Delta_f H^o$ (0 K) (H$^+$) = 1,528 kJ mol^{-1} [72], the enthalpy of formation of thioformaldehyde, $\Delta_f H^o$ (0 K) ($H_2C=S$) is found to amount to 114 ± 9 kJ mol^{-1}. This revised value is in good agreement with the value of 118 ± 8 kJ mol^{-1} at 0 K reported by Ruscic and Berkowitz [73] and is also supported by the theoretical $\Delta_f H^o$ (298 K) of 113.2 ± 4.2 kJ mol^{-1} reported by Kieninger and Ventura [74]. In this work, we opted to validate our calculated data solely upon the more recent experimental data of Ruscic and Berkowitz [73].

Mean absolute deviations between the experimental and ab initio calculated data for the various levels of theory and basis sets are presented in Fig. 3 for $\Delta_f H^o$ and in Fig. 4 for S^o. Detailed results can be found in Tables S-3 and S-4 of the supporting information.

From Fig. 3 it is seen that similar results are obtained with the 6-31g, 6-31++g and 6-311g basis sets. Both an increase of the valence basis set and addition of diffuse
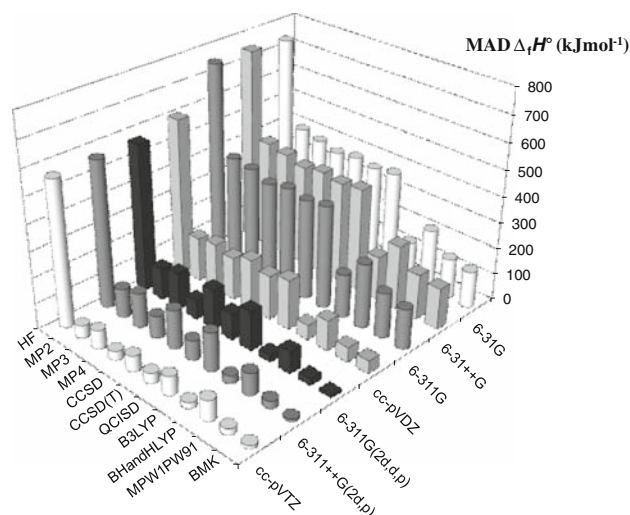
Fig. 3 Influence of the level of theory and basis set on the mean absolute deviation (MAD) between the ab initio and experimental standard enthalpies of formation at 298 K for the five compounds presented in Table 1
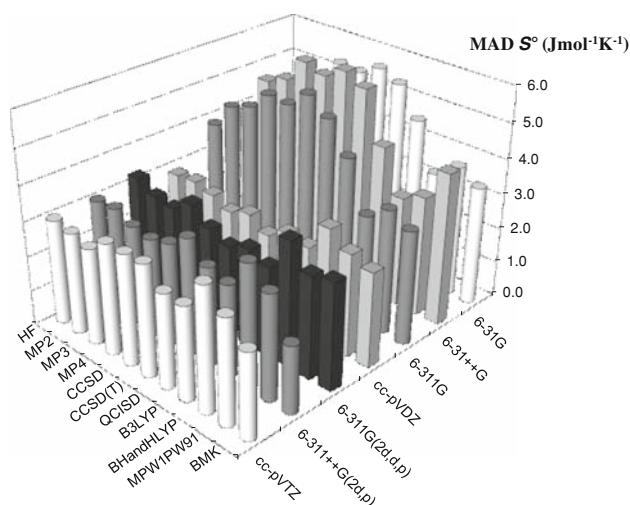
Fig. 4 Influence of the level of theory and basis set on the mean absolute deviation (MAD) between the ab initio and experimental standard molar entropies at 298 K for the five compounds presented in Table 1

functions hence do not significantly increase the agreement with the experimental standard enthalpies of formation. The minor influence of diffuse functions on the results is also shown by the coinciding 6-311++G(2d,p) and 6-311G(2d,d,p) values. With the non-polarized basis sets the HF MAD amounts to approximately 740 kJ mol^{-1}. Slightly better results for the same basis sets are obtained with the post-HF methods, yielding MADs in the range of 370 to 410 kJ mol^{-1}. DFT methods outperform their post-HF counterparts when using the non-polarized basis sets. With the 6-31G basis set, DFT methods yield MADs on $\Delta_f H^o$ varying between 130 and 230 kJ mol^{-1}.

The addition of polarization functions has a major influence on the calculated $\Delta_f H^o$ and largely enhances the accuracy of both the post-HF and DFT methods, lowering the MADs to approximately 110 and 40 kJ mol^{-1}, respectively. Amongst the post-HF and DFT methods, best results are obtained with the BMK/6-311G(2d,d,p) method yielding a MAD of 9.2 kJ mol^{-1}. It is observed that for the DFT methods similar results are obtained with the 6-311G(2d,d,p) basis set as with cc-pVTZ, while for the HF-based methods more accurate results are obtained with the cc-pVTZ basis set. High level MP4/cc-pVTZ or CCSD(T)/cc-pVTZ methods still overestimate the experimental standard enthalpies of formation with more than 30 kJ mol^{-1}. Even with the CCSD(T)/6-311G(3df,3pd) level of theory, the deviation between the calculated and experimental values does not drop below 10 kJ mol^{-1} for H_2S and $H_2C=S$ (see Fig. S-1 of the supporting information). Remaining errors are probably caused by basis set limitations and the limited electron correlation accounted for in these methods.

If more accurate energies are required, use has to be made of composite methods, such as G3, G3B3, CBS-QB3 and W1U. The Gaussian 3 methods account for basis set and electron correlation limitations by adding a set of basis set and electron correlation expansion corrections to MP4/6-31G(d) energy. CBS-QB3 counters basis set and electron correlation restrictions by extrapolating single point energies to the unreachable limit of a complete basis set and full electron correlation. W1U in its turn represents an approximation of the basis set limit CCSD(T) energy. All high level single point calculations for most composite methods can be done on relatively small basis sets. Hence, the total CPU time required for these calculations remains limited, yielding an ideal trade-off between accuracy and computational efficiency. The MADs between the calculated and experimental standard enthalpies of formation obtained with the composite methods are presented in Fig. 5, where they are compared with the lowest MADs obtained with four DFT methods studied in this work. The lowest MADs for B3LYP, BHandHLYP and MPW1PW91 are obtained with the cc-pVTZ basis set while for the BMK

functional the best agreement with experiment is obtained with the 6-311G(2d,d,p) basis set. For the five sulfur compounds under study, G3, G3B3 and CBS-QB3 yield MADs on $\Delta_f H^o$ of respectively 3.9, 4.9 and 3.8 kJ mol^{-1}, closely followed by the W1U scheme for which the MAD amounts to 5.4 kJ mol^{-1}. The W1U method fails to accurately predict the $\Delta_f H^o$s of dimethylsulfide and -disulfide, underestimating the experimental values of both compounds with approximately 9 kJ mol^{-1}. The MP2 basis set extrapolation method (MP2/∞) reproduces the experimental data within 18.9 kJ mol^{-1}. This corresponds with an accuracy of 3.2 kJ mol^{-1} per bond, which is in good agreement with the postulated accuracy for this method [47]. In general, it can be concluded that with the composite methods, an improvement of the accuracy with almost one order of magnitude can be obtained as compared to high level post-HF/6-311G(2d,d,p) methods while an improvement with a factor 2 is obtainable compared to the most accurate DFT method [BMK/6-311G(2d,d,p)]. Gomes and da Silva [21] also showed that DFT methods are less suited for the estimation of enthalpies of formation, while composite methods succeed to reproduce the experimental data of sulfur compounds quite reasonably.

The components studied in this work permit to evaluate the performance of the different ab initio methods in predicting the reaction enthalpy for the isodesmic reaction $H_2S + CH_3SSCH_3 \rightarrow CH_3SCH_3 + HSSH$. As the number of bonds is kept the same in isodesmic reactions, low level ab initio methods already succeed to accurately predict the standard reaction enthalpy, $\Delta_r H^o$, for this type of reaction. Therefore, isodesmic reactions are a valuable tool to study the enthalpies of formation of unknown
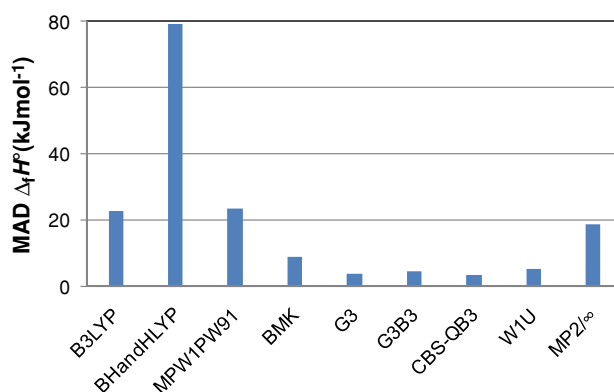
Fig. 5 Comparison between the MADs on the standard enthalpies of formation at 298 K obtained with the DFT and composite methods for the five compounds presented in Table 1. The minimum B3LYP, BHandHLYP and MPW1PW91 MADs are obtained with the cc-pVTZ basis set while for the BMK method the best agreement with experiment is obtained with the 6-311G(2d,d,p) basis set

compounds. In Table 2 the MADs between the experimental and calculated $\Delta_r H^o$s are presented. It is shown that all methods, with exception of HF, succeed to reproduce the experimental data quite accurately. Best agreement with the experimental $\Delta_r H^o$ is obtained with CCSD(T)/cc-pVDZ. The non-polarized basis sets perform surprisingly good for this reaction. For example, with the 6-311G basis set, a deviation of less than 1 kJ mol^{-1} is obtained for both the MP3, MP4, CCSD(T), MPW1PW91 and BMK method.

Standard molar entropies for the five compounds presented in Table 1 were calculated within the harmonic oscillator (HO) approximation. However in the HO model, special attention has to be given to the internal rotation around the S–S bond in disulfides. The S–H respectively the S–C bonds in HSSH and CH$_3$SSCH$_3$ are nearly at right angles, existing in a right- and left-hand form [51]. Within the HO approximation internal rotation around this S–S bond is forbidden, making one of the two forms inaccessible. For this reason the calculated HO entropy has to be augmented with $R\ln(2)$ [75]. The barrier for rotation around the S–S bond amounts to 25 kJ mol^{-1} (see Fig. S-2 of the supporting information). Due to the high barrier for rotation, the HO approximation succeeds to predict the contribution to the entropy of this internal rotation quite accurately at low temperatures. At 298 K, treatment of the S–S bond as a hindered rotor according to the procedure developed by Van Speybroeck et al. [76] increases the standard molar entropies with merely 0.4 and 0.3 J mol^{-1} K^{-1} for respectively HSSH and CH$_3$SSCH$_3$.

From Fig. 4 it is seen that for the standard molar entropies similar results are obtained with the 6-31G, 6-31++G and 6-311G basis sets. Only for the BMK functional an influence of diffuse functions on the calculated entropies is observed. With the 6-31G, 6-31++G and 6-311G basis sets, the best results are obtained with the DFT methods. With these basis sets, MADs ranging between 3 and 4 J mol^{-1} K^{-1} are obtained for the DFT methods while MADs ranging between 5 and 6 J mol^{-1} K^{-1} are obtained for the post-HF methods. Addition of polarization functions does significantly increase the agreement with experimental data in case of the post-HF methods. However for some DFT methods, such as BHandHLYP, the polarized basis sets yield similar results as their non-polarized counterparts. Figure 4 also shows that with the cc-pVDZ basis set slightly better agreement with experiment is obtained than with cc-pVTZ. The BMK/6-311++G(2d,p) method succeeds to reproduce the experimental data most accurately, yielding a MAD of 1.9 J mol^{-1} K^{-1}. Half of this MAD is due to an overestimation of the standard entropy of HSSH with 5.5 J mol^{-1} K^{-1} as compared to the experimental value of 252.4 J mol^{-1} K^{-1} [91]. All studied ab initio methods overestimate the standard entropy of this compound with at least 5 up to 12 mol^{-1} K^{-1}. This discrepancy is not due to the geometries used as the geometrical data for HSSH in this work are in agreement with the data reported by Zhou et al. [77] and Steudel et al. [78]. Moreover, the calculated standard molar entropies for HSSH ranging between 257 and 265 J mol^{-1} K^{-1} are in good agreement with the experimental value of 260 mol^{-1} K^{-1} reported by Benson [10]. Based on MP2/6-311++G** geometries and experimental frequencies, Migdisov et al. [79] estimated the entropy of HSSH to amount to 258.2 J mol^{-1} K^{-1}, which corresponds with the values obtained in this work.

Table 2 Mean absolute deviation (MAD) between the experimental and the calculated standard reaction enthalpies for the isodesmic reaction $H_2S + CH_3SSCH_3 \rightarrow CH_3SCH_3 + HSSH$

	6-31g	6-31++g	6-311g	6-311g (2d,d,p)	6-311++g (2d,p)	cc-pVDZ	cc-pVTZ
HF	4.0	2.3	4.2	8.6	7.8	6.9	7.2
MP2	*0.2*	3.9	1.6	1.6	3.5	2.7	4.0
MP3	2.2	1.5	*0.8*	3.6	2.1	2.0	1.7
MP4	*0.8*	3.4	*0.4*			1.2	
CCSD	3.1	*0.6*	1.8	3.4	1.8	2.0	
CCSD(T)	1.7	2.6	*0.6*			*0.1*	
QCISD	2.7	1.1	1.3	3.1	1.4	1.7	
B3LYP	2.2	*0.8*	1.7	3.8	3.2	2.7	2.7
BHandHLYP	2.8	1.1	2.2	5.2	4.6	3.9	4.0
MPW1PW91	*0.9*	*0.6*	*0.5*	3.3	2.7	1.6	2.2
BMK	*0.3*	1.7	*0.7*	4.0	2.6	2.7	2.4

MADs smaller than 1 kJ mol^{-1} are italicized

3.3 Kinetics

Five reactions belonging to three different reaction families are studied in this work, i.e. the H abstraction reactions from H_2S by the hydrogen and methyl radical, the homolytic substitution reactions of hydrogen on dimethylsulfide and on dimethyldisulfide and the addition reaction of methyl on thioformaldehyde (see Table 3). For four of the studied reactions experimental rate coefficients could retrieved from the NIST Chemical Kinetics Database [80]. For the studied addition reaction only theoretically estimated kinetic parameters could be obtained. For this reaction, the high level W1//QCISD/6-31G(d) calculations performed by Coote et al. [26] can be used as benchmark.

3.3.1 Transition state geometries

The transition state structures for the hydrogen abstraction of H_2S by $H^\bullet$ (reaction 1), the homolytic substitution reaction of $H^\bullet$ on dimethylsulfide (reaction 3) and the addition of methyl on thioformaldehyde (reaction 5) are shown in Fig. 6. The values for a, b, α and β are strongly dependent on the level of theory used. Values for these parameters as function of the level of theory and basis set can be found in Tables 4, 5 and 6 for reactions 1, 3 and 5, respectively. As the studied transition states of reactions 3 and 5 contain three non-hydrogen atoms, some of the high level post-HF calculations with triple zeta basis sets proved to be computationally too expensive.

From Tables 4, 5 and 6 it is observed that some transition states could not be retrieved with the B3LYP, MPW1PW91 and BMK functional methods, in particular when the barrier for reaction is small. No transition states could be located with B3LYP/6-31G and B3LYP/6-311G for the H abstraction from H_2S by $H^\bullet$. For the addition of methyl to thioformaldehyde, transition states could not be retrieved at the B3LYP, MPW1PW91 and BMK level of theory with the 6-31G and 6-311G basis sets. Non polarized basis sets hence seem to be inadequate to describe the forming/breaking bonds in transition states. However, from Tables 4, 5 and 6 it is observed that for the HF and post-HF methods transition states were retrieved for all three of the studied reactions, even with the smaller non polarized basis sets. In literature, reports have been made concerning the systematical underestimation of reaction barriers for radical reactions by DFT methods [81, 82]. This underestimation of the DFT barrier is attributed both to self-interaction [83] as to failure of the generalized gradient approximations (GGAs) to accurately describe the exchange correlation interaction [84]. As DFT barriers are lower than barriers calculated with HF and post-HF, DFT methods will fail more quickly in yielding a proper transition state with smaller basis sets than HF and post-HF methods.

From Table 4 it is seen that the transition state geometry for the H abstraction reaction from H_2S by $H^\bullet$ (reaction 1) can vary significantly depending on the ab initio method used for the transition state optimization. In particular, the

Table 3 Rate coefficients for five reactions involving organosulfur compounds retrieved from the NIST Chemical Kinetics Database [92]

Reaction	References	T (K)	$k_{exp}(T)$ (m^3 mol^{-1} s^{-1})
H abstraction			
1 $H_2S + H^\bullet \rightarrow H_2 + HS$	1999PEN/HU [87]	400	1.4×10^6
2 $H_2S + CH_3^\bullet \rightarrow CH_4 + HS^\bullet$	1983ARI/ART [16]	400	8.8×10^3
Homolytic substitution			
3 $(CH_3)_2S + H^\bullet \rightarrow CH_3SH + CH_3^\bullet$	1979YOK/STR [12]	400	6.3×10^5
4 $(CH_3S)_2 + H^\bullet \rightarrow CH_3SH + SCH_3^\bullet$	1980EKW/JOD [13]	400	5.0×10^5
Addition			
5 $H_2C=S + CH_3^\bullet \rightarrow C_2H_5S^\bullet$	1985SHU/BEN [93]	700	$9.4 \times 10^{4*}$

* Theoretically estimated value

Fig. 6 Transition state structures for reactions 1, 3 and 5 presented in Table 3. Values for the parameters a, b, α and β for each of the studied ab initio methods can be found respectively in Tables 4, 5 and 6
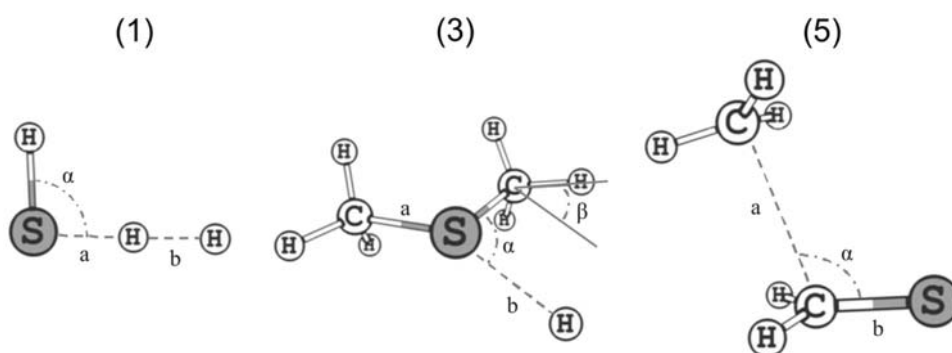
Table 4 Ab initio transition state geometries, imaginary frequencies and zero point corrected energy barriers for the hydrogen abstraction from H_2S by $H^\bullet$ (reaction **1**, Table 3)

Reaction **1**		a (pm)	b (pm)	α (°)	$Im(\nu^{\ddagger})$ (cm^{-1})	ΔE(0 K) (kJ mol^{-1})
HF and post-HF methods						
HF	6-31G	147	115	94.2	1,942	32.9
	6-311G	147	116	94.3	1,784	31.9
	6-311G(2d,d,p)	148	105	92.0	2,262	51.0
	cc-pVDZ	149	106	92.0	2,205	47.2
	cc-pVTZ	148	106	92.0	2,235	48.6
MP2	6-31G	147	116	93.5	1,777	29.6
	6-311G	147	116	93.9	1,594	27.5
	6-311G(2d,d,p)	146	105	91.0	1,806	32.9
	cc-pVDZ	146	107	90.8	1,735	29.8
	cc-pVTZ	145	106	90.3	1,722	27.0
	∞					24.3
PMP2	6-31G					19.0
	6-311G					17.2
	6-311G(2d,d,p)					20.8
	cc-pVDZ					18.1
	cc-pVTZ					14.8
MP3	6-31G	147	118	93.5	1,709	27.9
	6-311G	147	119	93.9	1,507	25.6
	6-311G(2d,d,p)	144	109	91.3	1689	28.8
	cc-pVDZ	145	111	91.0	1,592	25.8
	cc-pVTZ	144	110	90.8	1,584	22.6
MP4	6-31G	147	120	93.4	1,612	25.8
	6-311G	147	121	93.8	1,391	23.4
	6-311G(2d,d,p)	144	111	91.2	1,565	25.5
	cc-pVDZ	144	113	91.0	1,462	22.9
	cc-pVTZ	143	113	90.7	1,430	19.0
CCSD	6-31G	147	124	93.3	1,455	21.3
	6-311G	147	127	93.7	1,231	19.2
	6-311G(2d,d,p)	143	114	91.5	1,476	22.8
	cc-pVDZ	144	117	91.3	1,349	20.2
	cc-pVTZ	143	116	91.1	1,349	17.0
CCSD(T)	6-31G	147	124	93.3	1,433	20.9
	6-311G	146	127	93.7	1,197	18.7
	6-311G(2d,d,p)	143	115	91.4	1,391	21.1
	cc-pVDZ	144	118	91.1	1,275	18.8
	cc-pVTZ	142	117	90.9	1,240	14.8
QCISD	6-31G	147	124	93.3	1,450	21.1
	6-311G	146	127	93.7	1,223	19.1
	6-311G(2d,d,p)	143	114	91.5	1,475	22.7
	cc-pVDZ	144	117	91.2	1,359	20.1
	cc-pVTZ	143	116	91.1	1,353	16.9
DFT methods						
B3LYP	6-31G	×	×	×	×	×
	6-311G	×	×	×	×	×
	6-311G(2d,d,p)	138	142	92.2	488	2.4
	cc-pVDZ	138	154	92.1	316	0.4
	cc-pVTZ	138	146	92.2	427	1.5

Table 4 continued

Reaction **1**		a (pm)	b (pm)	α (°)	$\text{Im}(\nu^{\ddagger})$ (cm^{-1})	$\Delta E(0\text{ K})$ (kJ mol^{-1})
BHandHLYP	6-31G	140	146	94.4	496	1.4
	6-311G	140	151	94.4	423	3.0
	6-311G(2d,d,p)	140	122	92.2	956	8.1
	cc-pVDZ	141	127	92.2	800	5.2
	cc-pVTZ	140	124	92.3	898	6.7
MPW1PW91	6-31G	140	154	93.9	390	2.0
	6-311G	140	159	93.9	358	4.1
	6-311G(2d,d,p)	139	131	91.7	695	7.5
	cc-pVDZ	140	137	91.8	573	5.0
	cc-pVTZ	139	133	91.7	650	6.0
BMK	6-31G	142	145	93.9	570	6.8
	6-311G	142	149	94.0	603	9.4
	6-311G(2d,d,p)	142	127	91.6	918	14.2
	cc-pVDZ	142	135	91.9	797	10.6
	cc-pVTZ	141	130	91.7	866	12.7
Composite methods						
G3	–	104	148	91.4	2,331	12.2
G3B3	–	140	139	92.2	554	11.1
CBS-QB3	–	142	138	92.2	488	11.7
W1U	–	138	143	92.1	453	7.9

×, no transition state found for this level of theory; –, indicates that the calculation proved to be computationally too expensive

HF and post-HF transition states are much more shifted towards the product side, i.e. towards dihydrogen and hydrogenthiyl, compared to the DFT methods. All HF and post-HF methods predict a transitional S–H bond length around 146 pm and a forming H–H bond length ranging between 105 and 127 pm. This observation is in agreement with the findings of Kurosaki and Takayanagi [85]. In contrast to the HF based methods, the DFT methods predict a much earlier transition state: the S–H bond lengths range between 138 pm and 142 pm and the H–H bond lengths range from 122 up to 159 pm. Inclusion of polarization functions significantly shortens the H–H distance while the S–H bond length remains practically unchanged. It is observed from Table 4 that the influence of the level of theory on the transition state angles is small. All methods yield similar values for the bond angle α, ranging between 91 and 94°. For the composite methods, geometry optimizations are performed on the MP2/6-31G(d), B3LYP/6-31G(d), B3LYP/6-31G(2d,d,p) and B3LYP/cc-pV(T+d)Z level of theory for respectively G3, G3B3, CBS-QB3 and W1U. From Table 4 it can hence be seen that the geometry used in combination with the G3 scheme is in agreement with the geometries obtained with the HF methods, while the geometries used for the G3B3, CBS-QB3 and W1U methods are in excellent agreement with the DFT results.

The data presented in Tables 5 and 6 are in agreement with the reports of Zhang et al. [86] and Coote et al. [26]. From both tables, it is seen that analogous conclusions as for the H abstraction from H_2S by hydrogen can be drawn for the studied substitution (Table 5) and addition reaction (Table 6). The DFT methods predict much earlier transitions states as compared to the HF based methods. For the homolytic substitution of H$^{\bullet}$ on dimethylsulfide with the formation of methyl and methylmercaptane (reaction **3**), it is observed that the HF based methods yield forming S–H bond lengths that are shorter than their DFT equivalents, while the breaking S–C bond lengths are up to 10 pm longer. For the addition of methyl to thioformaldehyde (reaction **5**) it is observed that the forming C–C bonds obtained with DFT methods are on average 20 pm longer as compared to the HF based methods. As for reaction **1**, addition of polarization functions significantly influences the transitional bond lengths but has only a minor effect on the bond angles. The exception is the H–C–S–H dihedral angle in the transition state of reaction **3**. This angle is indicated as β in Fig. 6 and can change up to 30° by inclusion of polarization functions to the basis set. Due to the typical low energy barrier for addition reactions, transition states could not be retrieved for B3LYP, MPW1PW91 and BMK with the non-polarized basis sets for reaction **5**.

Table 5 Ab initio transition state geometries, imaginary frequencies and zero point corrected energy barriers for the homolytic substitution reaction of H$^\bullet$ on dimethylsulfide (reaction **3**, Table 3)

Reaction 3		a (pm)	b (pm)	α (°)	β (°)	Im($v^\ddagger$) (cm^{-1})	ΔE(0 K) (kJ mol^{-1})
HF and post-HF methods							
HF	6-31G	213	174	93.2	0.0	1,072	77.0
	6-311G	211	174	93.5	0.0	1,089	75.4
	6-311G(2d,d,p)	195	160	91.0	30.5	918	75.7
	cc-pVDZ	198	163	91.5	28.0	999	78.6
	cc-pVTZ	195	160	90.9	31.4	884	74.4
MP2	6-31G	210	164	92.5	17.4	1,152	86.0
	6-311G	209	164	92.3	26.9	1,117	79.2
	6-311G(2d,d,p)	189	162	88.4	36.7	627	46.1
	cc-pVDZ	196	154	89.1	37.1	383	56.0
	cc-pVTZ	188	163	88.1	34.8	565	37.1
	∞						28.3
PMP2	6-31G						61.7
	6-311G						55.5
	6-311G(2d,d,p)						34.0
	cc-pVDZ						41.4
	cc-pVTZ						24.8
MP3	6-31G	209	166	92.4	18.9	1,135	77.4
	6-311G	208	167	92.3	27.3	1,094	70.4
	6-311G(2d,d,p)	188	168	88.2	37.4	709	39.9
	cc-pVDZ	192	162	88.6	36.9	575	46.1
	cc-pVTZ	–	–	–	–	–	–
MP4	6-31G	210	166	92.1	22.2	1,066	72.8
	6-311G	209	167	91.9	30.3	1,021	65.6
	6-311G(2d,d,p)	–	–	–	–	–	–
	cc-pVDZ	192	165	88.2	36.8	549	40.0
	cc-pVTZ	–	–	–	–	–	–
CCSD	6-31G	212	172	91.8	25.1	905	59.9
	6-311G	210	174	91.7	30.7	866	53.3
	6-311G(2d,d,p)	189	171	88.2	37.0	622	32.6
	cc-pVDZ	192	167	88.5	36.3	574	37.8
	cc-pVTZ	–	–	–	–	–	–
CCSD(T)	6-31G	213	172	91.7	26.6	877	58.4
	6-311G	211	173	91.5	33.1	829	51.6
	6-311G(2d,d,p)	–	–	–	–	–	–
	cc-pVDZ	192	168	88.2	36.6	537	33.8
	cc-pVTZ	–	–	–	–	–	–
QCISD	6-31G	212	173	91.7	25.9	890	59.1
	6-311G	210	174	91.6	31.3	852	52.5
	6-311G(2d,d,p)	189	171	88.2	82.8	618	32.2
	cc-pVDZ	192	167	88.5	36.2	573	37.3
	cc-pVTZ	–	–	–	–	–	–
DFT methods							
B3LYP	6-31G	204	174	91.1	27.1	564	19.4
	6-311G	203	176	91.4	30.2	575	18.2
	6-311G(2d,d,p)	187	186	87.9	37.6	385	5.4
	cc-pVDZ	191	176	88.5	36.6	412	8.2
	cc-pVTZ	187	185	87.9	37.7	391	4.9

Table 5 continued

Reaction 3		a (pm)	b (pm)	α (°)	β (°)	$Im(\nu^{\ddagger})$ (cm^{-1})	ΔE(0 K) (kJ mol^{-1})
BHandHLYP	6-31G	204	169	93.0	8.8	750	32.5
	6-311G	203	171	93.2	13.7	752	31.3
	6-311G(2d,d,p)	187	171	88.7	35.0	526	17.8
	cc-pVDZ	192	165	89.3	34.9	512	22.6
	cc-pVTZ	187	170	88.7	35.3	505	17.3
MPW1PW91	6-31G	203	168	91.6	23.0	576	29.4
	6-311G	202	171	91.7	26.0	576	27.7
	6-311G(2d,d,p)	184	188	87.6	36.5	372	11.4
	cc-pVDZ	188	174	88.4	35.1	376	15.3
	cc-pVTZ	184	186	87.5	36.2	369	10.7
BMK	6-31G	205	164	91.8	21.8	575	40.0
	6-311G	204	167	91.8	26.3	563	39.5
	6-311G(2d,d,p)	188	180	87.6	36.9	583	21.6
	cc-pVDZ	190	179	88.1	36.9	532	22.6
	cc-pVTZ	188	182	87.6	37.4	558	20.9
Composite methods							
G3	–	201	148	90.3	36.3	1,081	7.9
G3B3	–	190	175	88.5	33.8	471	19.0
CBS-QB3	–	187	186	87.9	37.6	385	19.2
W1U	–	190	185	87.5	39.2	352	11.5

×, no transition state found for this level of theory; –, indicates that the calculation proved to be computationally too expensive

3.3.2 Reaction barriers and imaginary frequencies

Besides the influence of the level of theory on the transition state geometry, also the effect on the reaction barriers was investigated. The results of this study are presented in Tables 4, 5 and 6, respectively for reactions **1**, **3** and **5**. Besides energy barriers, also the imaginary frequencies of the transition state mode are given in these tables.

For the hydrogen abstraction from H$_2$S by H$^\bullet$ (reaction **1**), it is seen from Table 4 that large discrepancies are found between the energy barriers calculated with HF based, DFT and composite methods. The HF and post-HF methods yield barriers ranging between 14 and 51 kJ mol^{-1}. For these methods, it is observed that lower energy barriers are obtained when larger basis sets are used or more electron correlation is implemented in the method. The smallest energy barrier, i.e. 14.8 kJ mol^{-1}, is hence obtained with the CCSDT(T)/cc-pVTZ method. The energy barrier obtained with the MP2 basis set extrapolation procedure developed by Truhlar [46] is also depicted in Table 4. This method yields an energy barrier of 24.3 kJ mol^{-1}, which is approximately 3 kJ mol^{-1} lower than the value obtained with MP2/cc-pVTZ. In contrast to the HF based methods, for DFT methods it is observed that larger basis sets correspond with higher energy barriers. With the non-polarized basis sets, barriers ranging from 0.4

to 6.8 kJ mol^{-1} are observed. Addition of polarization functions increases the energy barriers with 4 kJ mol^{-1} on average. The composite methods predict energy barriers between 7.9 and 12.2 kJ mol^{-1}. The activation barriers around 12 kJ/mol^{-1} obtained with G3, G3B3 and CBS-QB3 correspond well, while W1U predicts a barrier that is some 4 kJ mol^{-1} lower. The obtained energy barriers are in agreement with values reported in literature [85, 87]. Peng et al. [87] report barriers heights of 12 kJ mol^{-1} obtained at the QCISD(T,full)/cc-pVTZ level on MP2(full)/cc-pVTZ geometries. Karton et al. [88] reported W3 and W4 zero-point exclusive barriers for this reaction around 15 kJ mol^{-1}, in good agreement with the barriers obtained with the G3, G3B3 and CBS-QB3 methods. From Table 4 it is seen that best agreement with the composite methods is obtained using the BMK method. The good agreement between BMK and complete basis set results was also shown for hydrogen abstraction reactions between hydrocarbons [56]. Post-HF methods systematically over-estimate the reaction barriers obtained with the composite methods. However, when high level methods are used combined with large basis sets, it is observed that the G3, G3B3 and CBS-QB3 energy barriers can be approached within 3 kJ mol^{-1}.

For the studied substitution reaction (reaction **3**, Table 5) the HF based methods yield barriers ranging

Table 6 Ab initio transition state geometries, imaginary frequencies and zero point corrected energy barriers for the addition of methyl on thioformaldehyde (reaction **5**, Table 3)

Reaction 5		a (pm)	b (pm)	α (°)	$\text{Im}(v^{\ddagger})$ (cm^{-1})	ΔE(0 K) (kJ mol^{-1})
HF and post-HF methods						
HF	6-31G	252	172	105.7	205	−5.9
	6-311G	248	171	106.1	228	−1.1
	6-311G(2d,d,p)	239	166	106.0	306	18.5
	cc-pVDZ	241	167	105.8	294	14.8
	cc-pVTZ	240	166	105.8	295	16.9
MP2	6-31G	267	167	109.4	148	58.9
	6-311G	262	166	110.8	169	57.8
	6-311G(2d,d,p)	248	160	109.1	308	50.8
	cc-pVDZ	251	161	108.5	278	50.6
	cc-pVTZ	251	160	109.4	268	48.5
	∞					46.0
PMP2	6-31G					21.0
	6-311G					20.8
	6-311G(2d,d,p)					17.4
	cc-pVDZ					16.5
	cc-pVTZ					15.0
MP3	6-31G	266	167	109.2	147	46.6
	6-311G	262	166	110.1	162	44.5
	6-311G(2d,d,p)	248	161	108.5	294	42.6
	cc-pVDZ	251	162	107.9	267	42.5
	cc-pVTZ	252	161	108.7	251	40.2
MP4	6-31G	266	167	109.6	155	55.5
	6-311G	262	166	111.0	170	54.2
	6-311G(2d,d,p)	–	–	–	–	–
	cc-pVDZ	–	–	–	–	–
	cc-pVTZ	–	–	–	–	–
CCSD	6-31G	250	171	107.9	329	19.8
	6-311G	249	170	108.6	324	19.1
	6-311G(2d,d,p)	246	164	107.7	334	21.6
	cc-pVDZ	247	165	107.3	336	21.6
	cc-pVTZ	–	–	–	–	–
CCSD(T)	6-31G	253	171	108.0	307	20.2
	6-311G	252	170	108.7	299	19.2
	6-311G(2d,d,p)	–	–	–	–	–
	cc-pVDZ	–	–	–	–	–
	cc-pVTZ	–	–	–	–	–
QCISD	6-31G	249	171	107.8	337	19.8
	6-311G	248	170	108.4	329	19.0
	6-311G(2d,d,p)	246	164	107.7	327	20.9
	cc-pVDZ	247	165	107.2	327	20.8
	cc-pVTZ	–	–	–	–	–
DFT methods						
B3LYP	6-31G	×	×	×	×	×
	6-311G	×	×	×	×	×
	6-311G(2d,d,p)	269	163	110.4	125	7.1
	cc-pVDZ	274	163	110.3	107	5.6
	cc-pVTZ	269	163	110.0	134	8.2

Table 6 continued

Reaction **5**		a (pm)	b (pm)	α (°)	$Im(\nu^{\ddagger})$ (cm^{-1})	$\Delta E(0\ K)$ (kJ mol^{-1})
BHandHLYP	6-31G	289	166	111.2	55	2.3
	6-311G	276	165	110.9	93	4.8
	6-311G(2d,d,p)	256	162	108.7	204	12.1
	cc-pVDZ	260	163	108.5	186	10.1
	cc-pVTZ	257	162	108.5	201	12.4
MPW1PW91	6-31G	×	×	×	×	×
	6-311G	×	×	×	×	×
	6-311G(2d,d,p)	273	161	110.7	108	5.7
	cc-pVDZ	276	162	110.0	104	5.0
	cc-pVTZ	275	161	110.4	109	6.4
BMK	6-31G	×	×	×	×	×
	6-311G	×	×	×	×	×
	6-311G(2d,d,p)	265	163	110.2	42	8.1
	cc-pVDZ	306	162	114.9	137	2.3
	cc-pVTZ	267	162	109.9	97	8.4
Composite methods						
G3	–	250	161	109.0	253	17.5
G3B3	–	291	163	112.7	33	5.5
CBS-QB3	–	269	163	110.4	125	4.9
W1U	–	267	162	109.9	140	6.6
Other work						
Coote et al. [26]						13.7

×, no transition state found for this level of theory; –, indicates that the calculation proved to be computationally too expensive

between 32 and 86 kJ mol^{-1}. Much lower barriers are obtained with the DFT and composite methods which both predict barrier heights around 20 kJ mol^{-1}. For the addition of methyl to thioformaldehyde (reaction **5**, Table **6**), large discrepancies are observed between the perturbative methods on the one hand and coupled cluster/quadratic configuration methods on the other hand. The Møller–Plesset methods predict barriers from 40 up to 50 kJ mol^{-1} while the coupled cluster methods and QCISD predict a barrier around 20 kJ mol^{-1}. The DFT methods and composite methods predict barriers ranging from a few kJ mol^{-1} up to 20 kJ mol^{-1}. For both reactions **3** and **5**, it is observed that the DFT methods succeed to reproduce more accurately the results obtained with the composite methods. Post-HF methods yield smaller energy barriers when larger basis sets are used and more electron correlation is included in the method. For reaction **3**, the MP2/∞ barrier (28.1 kJ mol^{-1}) differ significantly from the one obtained with MP2/cc-pVTZ (37.1 kJ mol^{-1}). A large basis set proves to be very important to accurately predict the reaction barrier for this type of reaction. For reaction **5**, the deviation between the MP2/cc-pVTZ and MP2/∞ barrier amounts to 2 kJ mol^{-1} only. For the homolytic substitution reaction (Table **5**) the G3 method predicts a

barrier of 7.9 kJ mol^{-1}, while G3B3 and CBS-QB3 predict barriers that are 11 kJ mol^{-1} higher. The W1U method predicts a barrier of 11.5 kJ mol^{-1}, which is in between the values obtained with G3 and CBS-QB3. For the studied addition reaction (Table **6**) it is observed that the G3 barrier is some 12 kJ mol^{-1} higher than the G3B3, CBS-QB3 and W1U barriers. This can be attributed to the different geometries used for the single point calculations. As mentioned above, the G3 method uses MP2/6-31G(d) geometries while the G3B3, CBS-QB3 and W1U schemes make use of DFT geometries. Coote et al. [26] reported that DFT methods are probably less suited for predicting the transition states of addition reactions to C=S double bonds. As MPW1K and B3LYP do not succeed to accurately predict the transition state geometries, the authors found that high level single points calculations [CCSD(T)/6-311+G(d,p)] performed on these faulty DFT transition states inevitably led to an underestimation of the reaction barrier. Consequently, both the CBS-QB3, G3B3 and W1U barriers are lower than those obtained with G3 for the studied addition reaction. Similar conclusion were drawn by Saeys et al. [50] who studied hydrogen addition reactions to carbon-carbon double bonds. Based on high level W1 calculations on the QCISD/6-31G(d) transition state

geometry, Coote et al. [26] suggest a barrier of 13.7 kJ mol^{-1} for this reaction. The BHandHLYP/cc-pVTZ method succeeds to reproduce this barrier up to 1 kJ mol^{-1}. The composite methods W1U, CBS-QB3 and G3B3 underestimate the barrier by 9 kJ mol^{-1} while for the BMK cc-pVTZ method this underestimation amounts to some 5 kJ mol^{-1}.

For all three reactions, large discrepancies between the energy barriers obtained with the post-HF and composite methods were observed. A part of the overestimation can probably be attributed to spin contamination. Contamination of the transition state wave function by higher energy spin states can seriously increase the energy barrier, especially for perturbative methods. For the studied H abstraction reaction, the HF based methods predict a total spin ranging between 0.78 and 0.79, which is close to the theoretical value of 0.75. For the substitution reaction of H$^{\bullet}$ on DMS (reaction **3**) and in particular for the addition reaction of methyl to thioformaldehyde (reaction **5**), spin contamination becomes significant. For reactions **3** and **5**, total spin values obtained with the HF based methods vary around respectively 0.83 and 1.1. This pertains to an overestimation of the actual spin state with 16 and 46 percent. For these two reactions, spin contamination can hence be expected to have an important influence on the calculated energy barriers. This is also shown in Tables 4, 5 and 6 where the spin project MP2 (PMP2) energy barriers are presented. Correcting for spin contamination lowers the reaction barrier for reactions **1**, **3** and **5** with respectively 11, 17 and 35 kJ mol^{-1}. The PMP2 energy barriers approach the values obtained with the composite methods within 10 kJ mol^{-1}. Compared to HF based methods, DFT methods suffer much less from spin contamination. DFT spin values range between approximately 0.75 for reaction **1** to 0.80 for reaction **5**.

From Tables 3, 4 and 5 it can also be seen that the HF based methods predict much higher imaginary frequencies compared to the DFT methods. In general, these higher imaginary frequencies correspond with higher energy barriers. For the studied H abstraction, substitution and addition reaction, HF based imaginary frequencies fluctuate respectively around 1,700, 1,000 and 200 cm^{-1}, while DFT imaginary frequencies vary respectively around 500, 500 and 100 cm^{-1}. The lower imaginary frequencies obtained for the addition of methyl to thioformaldehyde (reaction **3**) are due to the higher reduced mass for motion along the reaction coordinate.

3.3.3 Rate coefficients

Rate coefficients for the five reactions presented in Table 3 have been calculated using classical transition state theory and are presented in Table 7. Besides rate coefficients, also the arithmetic and geometric mean ρ values for the studied reactions can be retrieved in Table 7.

For the hydrogen abstraction from H$_2$S by H (reaction **1**) the calculated rate coefficients are in relatively good agreement with the experimental value of 1.4×10^6 m^3 mol^{-1} s^{-1}. The lower level post-HF methods yield rate coefficients around 5×10^4 m^3 mol^{-1} s^{-1}, while CCSD, CCSD(T) and QCISD methods yield rate coefficients ranging from 1×10^5 up to 1.1×10^6 m^3 mol^{-1} s^{-1}. The DFT methods and composite methods slightly overestimate the experimental value predicting rate coefficients ranging between 1×10^6 up to 7×10^7 m^3 mol^{-1} s^{-1}. For the hydrogen abstraction from H$_2$S by methyl (reaction **2**), it is observed that all of the studied methods, with exception of HF and B3LYP, succeed to reproduce the experimental rate coefficient of 8.8×10^3 m^3 mol^{-1} s^{-1} within a factor 10. For the two homolytic substitution reactions (reactions **3** and **4**), the non-spin-projected HF methods systematically underestimate the experimentally observed rate coefficients. For these methods the calculated rate coefficients range from 1×10^{-1} to 2.3×10^3 m^3 mol^{-1} s^{-1} and from 3×10 to 4×10^5 m^3 mol^{-1} s^{-1} for reactions **3** and **4** respectively, while the experimental values amount to 6.3×10^5 and 5.0×10^5 m^3 mol^{-1} s^{-1}. For reaction **3** the results obtained with the DFT and composite methods are in good agreement with experiment. For reaction **4** it is observed that the DFT and composite methods tend to slightly overestimate the experimental value, yielding rate coefficients ranging from 7×10^6 up to 1×10^8 m^3 mol^{-1} s^{-1}. High level calculations for the addition of methyl to thioformaldehyde point towards a rate coefficient of 1.3×10^5 m^3 mol^{-1} s^{-1} [26]. For this reaction, the CCSD, CCSD(T) and QCISD method predict rate coefficients around 5×10^4 m^3 mol^{-1} s^{-1}, while the perturbative methods yield rate coefficients that are two orders of magnitude smaller. The DFT methods and composite methods (with exception of G3) predict values ranging from 2×10^5 up to 1×10^7 m^3 mol^{-1} s^{-1}.

From the $\langle \rho \rangle$ values presented in Table 7, it is observed that the agreement between the (post-)HF rate coefficients and experimental data is generally rather poor. However, the calculated rate coefficients tend to approach the experimental values when larger basis sets are used and when more electron correlation is accounted for. For example with the MP2 method, $\langle \rho \rangle_{\text{arithm}}$ values are obtained ranging between 10^2 on the cc-pVTZ basis set and 10^8 on 6-31G, indicating that the relative difference between calculated and experimental data amounts up to eight orders of magnitude. These large $\langle \rho \rangle$ values are mainly caused by a strong underestimation of the rate coefficients for the substitution reactions of hydrogen on dimethylsulfide and on dimethyldisulfide (reactions **3** and **4**). For both reactions, it is observed that all HF based methods underestimate the rate coefficients with at least a

Table 7 Ab initio rate coefficients for the five reactions presented in Table 3

		k (m^{3}mol^{-1} s^{-1})					$\langle\rho\rangle_{\mathrm{arithm}}$	$\langle\rho\rangle_{\mathrm{geom}}$
Reaction nr.:		**1**	**2**	**3**	**4**	**5**		
T:		400	400	400	400	700		
Experiment:		1.4×10^6	8.8×10^3	6.3×10^5	5.0×10^5	(9.4×10^4)		
HF and post-HF methods								
HF	6-31G	1.5×10^4	3.1×10^2	2.7×10^{-2}	2.5×10^5	5.2×10^6	6.9×10^6	2.2×10^4
	6-311G	1.5×10^4	8.0×10	4.1×10^{-2}	4.8×10^4	1.9×10^6	3.8×10^6	2.1×10^3
	6-311G(2d,d,p)	2.2×10^2	1.3×10^{-1}	1.5×10^{-2}	3.5×10	3.3×10^4	1.1×10^7	2.7×10^5
	cc-pVDZ	5.7×10^2	5.4×10^{-1}	8.8×10^{-3}	4.4×10	6.3×10^4	1.8×10^7	1.6×10^5
	cc-pVTZ	4.3×10^2	1.6×10^{-1}	2.0×10^{-2}	3.0×10	5.2×10^4	8.1×10^6	2.0×10^5
MP2	6-31G	2.7×10^4	4.2×10^4	2.3×10^{-3}	3.0×10^2	3.2×10	6.7×10^7	6.8×10^3
	6-311G	3.7×10^4	6.7×10^4	1.2×10^{-2}	4.1×10^2	1.1×10^2	1.3×10^7	4.4×10^3
	6-311G(2d,d,p)	1.1×10^4	3.6×10^3	5.1×10	1.0×10^4	1.5×10^2	3.3×10^3	2.3×10^2
	cc-pVDZ	2.6×10^4	8.8×10^2	2.4	3.8×10^3	1.7×10^2	6.7×10^4	7.5×10^2
	cc-pVTZ	5.8×10^4	1.7×10^4	7.2×10^2	4.1×10^4	3.3×10^2	2.7×10^2	5.2×10
PMP2	6-31G	4.9×10^5	4.2×10^4	3.4	5.9×10^5	7.9×10^4	4.6×10^4	7.8×10
	6-311G	6.7×10^5	6.7×10^4	1.5×10	4.8×10^5	6.2×10^4	1.1×10^4	6.0×10
	6-311G(2d,d,p)	3.3×10^5	3.6×10^3	2.0×10^3	3.7×10^5	4.6×10^4	8.7×10	1.6×10
	cc-pVDZ	6.7×10^5	8.8×10^2	1.9×10^2	1.6×10^5	5.9×10^4	8.4×10^2	4.3×10
	cc-pVTZ	1.6×10^6	1.7×10^4	2.9×10^4	1.2×10^6	1.0×10^5	*7.6*	*4.1*
MP3	6-31G	4.0×10^4	2.0×10^4	2.6×10^{-2}	9.4×10^2	1.0×10^3	6.0×10^6	2.1×10^3
	6-311G	5.8×10^4	1.1×10^4	1.5×10^{-1}	1.5×10^3	1.2×10^3	1.0×10^6	9.6×10^2
	6-311G(2d,d,p)	3.1×10^4	1.1×10^3	3.8×10^2	2.7×10^4	6.6×10^2	5.0×10^2	1.1×10^2
	cc-pVDZ	6.8×10^4	2.1×10^3	5.2×10	1.2×10^4	7.4×10^2	3.2×10^3	1.6×10^2
	cc-pVTZ	1.7×10^5	4.4×10^3	–	–	1.5×10^3	*5.1*	*4.1*
MP4	6-31G	6.3×10^4	1.1×10^4	8.3×10^{-2}	–	–	2.5×10^6	5.9×10^2
	6-311G	9.4×10^4	7.2×10^3	6.0×10^{-1}	–	–	3.5×10^5	2.7×10^2
	6-311G(2d,d,p)	6.7×10^4	–	–	–	–	2.1×10	2.1×10
	cc-pVDZ	1.3×10^5	–	3.3×10^2	–	–	9.5×10^2	1.4×10^2
	cc-pVTZ	3.8×10^5	–	–	–	–	*3.6*	*3.6*
CCSD	6-31G	1.9×10^5	4.6×10^4	3.1	3.8×10^5	4.9×10^4	5.1×10^4	1.1×10^2
	6-311G	2.7×10^5	2.9×10^4	1.8×10	3.1×10^5	5.1×10^4	8.6×10^3	5.9×10
	6-311G(2d,d,p)	1.3×10^5	1.8×10^3	3.2×10^3	–	2.5×10^4	7.0×10	2.1×10
	cc-pVDZ	2.6×10^5	3.9×10^3	6.9×10^2	1.1×10^5	2.5×10^4	2.4×10^2	2.9×10
	cc-pVTZ	6.4×10^5	5.5×10^3	–	–	–	*1.9*	*1.8*
CCSD(T)	6-31G	2.1×10^5	1.7×10^5	4.4	–	5.9×10^4	4.8×10^4	2.6×10^2
	6-311G	3.1×10^5	3.7×10^3	2.4×10	–	6.3×10^4	8.9×10^3	6.6×10
	6-311G(2d,d,p)	2.0×10^5	–	–	–	–	*7.0*	*7.0*
	cc-pVDZ	3.6×10^5	1.6×10^3	2.3×10^3	–	–	9.5×10	1.8×10
	cc-pVTZ	1.1×10^6	–	–	–	–	*1.3*	*1.3*
QCISD	6-31G	2.0×10^5	5.7×10^4	3.7	–	4.6×10^4	5.7×10^4	2.0×10^2
	6-311G	2.9×10^5	3.5×10^4	2.3×10	–	5.0×10^4	9.3×10^3	8.1×10
	6-311G(2d,d,p)	1.4×10^5	2.0×10^3	3.7×10^3	–	2.8×10^4	6.1×10	1.9×10
	cc-pVDZ	2.6×10^5	4.4×10^3	8.0×10^2	–	2.9×10^4	2.6×10^2	2.0×10
	cc-pVTZ	6.6×10^5	6.2×10^3	–	–	–	*1.8*	*1.7*

Table 7 continued

		k (m^{3}mol^{-1} s^{-1})					$\langle\rho\rangle_{\mathrm{arithm}}$	$\langle\rho\rangle_{\mathrm{geom}}$
Reaction nr.:		**1**	**2**	**3**	**4**	**5**		
T:		400	400	400	400	700		
Experiment:		1.4×10^6	8.8×10^3	6.3×10^5	5.0×10^5	(9.4×10^4)		
DFT methods								
B3LYP	6-31G	$\times$	$\times$	2.8×10^5	$\times$	$\times$	*2.3*	*2.3*
	6-311G	$\times$	5.2×10^6	4.2×10^5	$\times$	$\times$	2.9×10^2	3.0×10
	6-311G(2d,d,p)	3.1×10^7	1.9×10^5	1.1×10^7	$\times$	9.9×10^5	2.1×10	2.1×10
	cc-pVDZ	7.1×10^7	7.3×10^5	4.7×10^6	$\times$	1.7×10^6	4.8×10	3.2×10
	cc-pVTZ	4.5×10^7	$2.1 \times \times 10^5$	1.3×10^7	$\times$	9.6×10^5	2.6×10	2.5×10
BHandHLYP	6-31G	3.3×10^7	1.4×10^6	1.8×10^4	4.7×10^7	9.4×10^6	5.6×10	3.3×10
	6-311G	2.4×10^7	5.3×10^5	1.9×10^4	3.0×10^7	2.3×10^6	2.9×10	2.1×10
	6-311G(2d,d,p)	5.6×10^6	8.4×10^3	2.6×10^5	7.1×10^6	2.2×10^5	*2.2*	*1.9*
	cc-pVDZ	1.3×10^7	3.6×10^4	6.5×10^4	7.1×10^6	3.7×10^5	*6.1*	*4.7*
	cc-pVTZ	8.6×10^6	1.7×10^4	3.0×10^5	7.4×10^6	2.5×10^5	*2.9*	*2.4*
MPW1PW91	6-31G	3.2×10^7	$\times$	1.6×10^4	3.6×10^7	$\times$	2.3×10	1.9×10
	6-311G	1.9×10^7	7.6×10^6	2.6×10^4	2.2×10^7	$\times$	2.3×10^2	3.3×10
	6-311G(2d,d,p)	6.5×10^6	1.9×10^5	1.9×10^6	1.3×10^7	1.6×10^6	*8.0*	*5.3*
	cc-pVDZ	1.4×10^7	5.6×10^5	5.5×10^5	1.2×10^7	2.3×10^6	1.9×10	*6.5*
	cc-pVTZ	1.1×10^7	2.4×10^5	2.3×10^6	1.7×10^7	1.9×10^6	1.0×10	*7.1*
BMK	6-31G	8.3×10^6	$\times$	7.2×10^2	7.6×10^6	$\times$	2.9×10^2	1.9×10
	6-311G	4.1×10^6	9.0×10^5	6.3×10^2	2.7×10^6	$\times$	2.8×10^2	2.9×10
	6-311G(2d,d,p)	9.8×10^5	2.6×10^4	9.1×10^4	1.8×10^6	5.0×10^5	*3.6*	*3.1*
	cc-pVDZ	3.4×10^6	1.6×10^5	5.8×10^4	1.7×10^6	6.3×10^6	*8.7*	*6.5*
	cc-pVTZ	1.6×10^6	3.2×10^4	9.8×10^4	1.5×10^6	6.6×10^5	*3.9*	*3.3*
Composite methods								
G3	–	4.4×10^6	3.2×10^4	1.8×10^7	9.9×10^7	4.8×10^4	1.4×10	*9.0*
G3B3	–	1.8×10^6	7.6×10^3	2.0×10^5	$\times$	6.0×10^6	*1.9*	*1.7*
CBS-QB3	–	2.0×10^6	3.2×10^4	1.8×10^5	$\times$	1.4×10^6	*2.9*	*2.7*
W1U	–	3.0×10^6	2.1×10^4	8.7×10^5	$\times$	4.5×10^5	*2.0*	*1.9*
Other work								
Coote et al. [26][a]						1.3×10^5		

$\langle\rho\rangle$ values smaller than 10 are italicized

The $\langle\rho\rangle$ values represent the mean deviation between experimental and ab initio data for reaction **1** to **4**

$\times$, no transition state found for this level of theory; –, indicates that the calculation proved to be computationally too expensive

[a] Rate coefficients based on the W1//QCISD/6-31G(d) results reported by the authors

factor 17. However, when the spin projected energies and sufficient large basis sets are used, rate coefficients can be obtained well within a factor 10 of the experimental data. Consequently, PMP2/cc-pVTZ outperforms all other HF based methods. This method succeeds to reproduce the experimental rate coefficients of reactions **1**, **2**, **3** and **4** within a factor 4. Despite the large discrepancies between experiment and theory for reactions **3** and **4**, the high level post-HF methods succeed to accurately predict the rate coefficients for the studied H abstraction reactions (reactions **1** and **2**). The CCSD/cc-pVTZ method reproduces the

rate coefficients for both reactions within a factor 2 while the CCSD(T)/cc-pVTZ method reproduces the experimental rate coefficient of reaction **1** within 30%.

For DFT and composite methods the average deviation between the calculated and experimental rate coefficients fluctuates around a factor 10. The disadvantage of the DFT methods is that some of them sometimes fail to yield a proper transition state for low barrier reactions. For the homolytic substitution of hydrogen on dimethyldisulfide, transition states could not be retrieved with the B3LYP functional, independent of the basis set used. Best results

are obtained with the BHandHYLP method which reproduces the experimental rate coefficients within a factor 2. Similar accuracies are also obtained with the G3B3, CBS-QB3 and W1U method. However, these three composite methods rely on the B3LYP method for finding a transition state and could not yield rate coefficients for reaction **4**. The BMK functional, the G3 method and MPW1PW91 functional also prove to yield rather accurate rate coefficients, yielding $\langle \rho \rangle_{geom}$ values of respectively 3, 5 and 9. For reaction **5**, it is observed that the BHandHLYP/cc-pVTZ and PMP2/cc-pVTZ methods succeed to reproduce the W1 results reported by Coote et al. [26] the best. Also the post-HF methods succeed to reproduce this value quite well, i.e. within a factor 10. The composite methods that make use of B3LYP optimizations tend to slightly overestimate the rate coefficient for reaction **5**: W1U, CBS-QB3 and G3B3 yield rate coefficients that are respectively a factor 3, 11 and 46 higher.

4 Conclusions

Polarization functions are indispensable for the accurate prediction of geometries for organosulfur compounds. Addition of 2d, d and p polarization functions for respectively S, C and H reduces the mean absolute deviation between experimental and theoretical bond lengths to 2 pm. When post-HF methods are used, slightly higher accuracies can be obtained with the cc-pVTZ basis set, due to a better description of the S–S bond length. Addition of diffuse functions and extra valence functions has only a minor influence on the calculated geometries.

The best agreement with experimental standard enthalpies of formation is obtained with the CBS-QB3 and G3 method, both yielding MADs of approximately 4 kJ mol^{-1}. Surprisingly, the high level W1U composite method underestimates the experimental standard enthalpy of formation of dimethylsulfide and dimethyldisulfide with 9 kJ mol^{-1}. Post-HF methods require extensive basis sets in order to yield accurate standard enthalpies of formation. The MP4/cc-pVTZ and CCSD(T)/cc-pVTZ methods still overestimate the experimental standard enthalpies of formation with more than 30 kJ mol^{-1}. The BMK functional proves to be a low-cost alternative for the more computational demanding composite methods. When using the cc-pVTZ basis set, this functional reproduces the experimental enthalpies of formation within 10 kJ mol^{-1}.

Mean deviations between experimental and calculated standard entropies range between 2 and 6 J mol^{-1} K^{-1}. When small, non-polarized basis sets are used, best agreement with experimental data is obtained with the DFT methods. With polarized basis sets, all methods tend to

yield equally accurate standard entropies of formation, within 3 mol^{-1} K^{-1} of the experimental values.

Large discrepancies between DFT and HF transition state structures are noticed. DFT methods tend to predict a much earlier transition state compared to HF based methods. Using either DFT or HF transition states for high level single point calculations or extrapolation schemes can influence the calculated energy barriers with more than 10 kJ mol^{-1}. The best agreement with experimental rate coefficients for the studied reactions is obtained with the BHandHLYP/cc-pVTZ method. This DFT method allows to predict the experimental rate coefficients within a factor 2. This is slightly better than CBS-QB3, G3B3 and W1U which yield rate coefficients that deviate, on average, a factor 2 to 3 from the experimental data. However, the latter methods rely on the B3LYP method for finding a transition state, resulting in the fact that for some low barrier reactions no proper transition state can be found. HF and post-HF methods perform poorly in reproducing the experimental rate coefficients, underestimating for example the rate coefficient for the homolytic addition of hydrogen to dimethylsulfide with at least a factor 17. This underestimation of the rate coefficient is mainly caused by spin contamination of the transition state. The PMP2/cc-pVTZ method succeeds to approach the experimental rate coefficients within a factor 4.

Accurate, yet feasible thermochemical data for organosulfur compounds can be obtained with the commonly used composite methods such as G3, G3B3 and CBS-QB3. Among the studied DFT methods, only the BMK/cc-pVTZ method succeeds to reproduce the experimental standard enthalpies of formation within 10 kJ mol^{-1}. Most accurate rate coefficients are obtained using the BHandHLYP/cc-pVTZ method, closely followed by the composite methods and the BMK functional. The composite methods G3B3 and CBS-QB3 and the BMK/cc-pVTZ method thus prove to be powerful tools for an accurate prediction of both thermochemical and kinetic data for organosulfur compounds.

References

1. Hewitt CN (2001) Atmos Environ 35:1155. doi:10.1016/S1352-2310(00)00463-5
2. Shiraishi Y, Taki Y, Hirai T, Komasawa I (2001) Ind Eng Chem Res 40:1213. doi:10.1021/ie000547m
3. Shiraishi Y, Tachibana K, Taki Y, Hirai T, Komasawa I (2001) Ind Eng Chem Res 40:1225. doi:10.1021/ie000548e
4. Ma XL, Sprague M, Song CS (2005) Ind Eng Chem Res 44:5768. doi:10.1021/ie0492810

5. Bajus M, Baxa J (1985) Collect Czech Chem Commun 50:2903
6. Wang J, Reyniers MF, Marin GB (2007) Ind Eng Chem Res 46:4134. doi:10.1021/ie061096u
7. Mayadunne RTA, Rizzardo E, Chiefari J, Chong YK, Moad G, Thang SH (1999) Macromolecules 32:6977. doi:10.1021/ma9906837
8. den Hartog GJM, Haenen GRMM, Vegt E, van der Vijgh WJF, Bast A (2002) Biol Chem 383:709. doi:10.1515/BC.2002.073
9. Jiang JJ, Chang TC, Hsu WF, Hwang JM, Hsu LY (2003) Chem Pharm Bull (Tokyo) 51:1307. doi:10.1248/cpb.51.1307
10. Benson SW (1978) Chem Rev 78:23. doi:10.1021/cr60311a003
11. Luo YR (2003) Handbook of bond dissociation energies in organic compounds. CRC Press, Boca Raton
12. Yokota T, Strausz OP (1979) J Phys Chem 83:3196. doi:10.1021/j100488a003
13. Ekwenchi MM, Jodhan A, Strausz OP (1980) Int J Chem Kinet 12:431. doi:10.1002/kin.550120608
14. Ekwenchi MM, Safarik I, Strausz OP (1981) Int J Chem Kinet 13:799. doi:10.1002/kin.550130905
15. Arthur NL, Lee MS (1976) Aust J Chem 29:1483
16. Arican H, Arthur NL (1983) Aust J Chem 36:2195
17. Lendvay G, Berces T (1987) J Photochem Photobiol Chem 40:31
18. Ochterski JW, Petersson GA, Montgomery JA (1996) J Chem Phys 104:2598. doi:10.1063/1.470985
19. Curtiss LA, Raghavachari K, Redfern PC, Rassolov V, Pople JA (1998) J Chem Phys 109:7764. doi:10.1063/1.477422
20. Benassi R, Taddei F (1998) J Phys Chem A 102:6173. doi:10.1021/jp980927+
21. Gomes JRB, da Silva MAVR (2004) J Phys Chem A 108:11684. doi:10.1021/jp046993v
22. Fu Y, Lin BL, Song KS, Liu L, Guo QX (2002) J Chem Soc Perkin Trans 2:1223
23. Chandra AK, Nam PC, Nguyen MT (2003) J Phys Chem A 107:9182. doi:10.1021/jp035622w
24. Wright JS, Johnson ER, DiLabio GA (2001) J Am Chem Soc 123:1173. doi:10.1021/ja002455u
25. do Couto PC, Cabral BJC, Simoes JAM (2006) Chem Phys Lett 421:504. doi:10.1016/j.cplett.2006.02.009
26. Coote ML, Wood GPF, Radom L (2002) J Phys Chem A 106:12124. doi:10.1021/jp0267656
27. Henry DJ, Coote ML, Gomez-Balderas R, Radom L (2004) J Am Chem Soc 126:1732. doi:10.1021/ja039139a
28. Macrae RM, Carmichael I (2001) J Phys Chem A 105:3641. doi:10.1021/jp004170+
29. Izgorodina EI, Coote ML (2006) J Phys Chem A 110:2486. doi:10.1021/jp055158q
30. Benassi R (2004) Theor Chem Acc 112:95. doi:10.1007/s00214-004-0570-7
31. Mousavipour SH, Namdar-Ghanbari MA, Sadeghian L (2003) J Phys Chem A 107:3752. doi:10.1021/jp022291z
32. Pei KM, Li YM, Kong XL, Li HY (2003) Chin J Chem Phys 16:251
33. Chiu SW, Lau KC, Li WK (2000) J Phys Chem A 104:3028. doi:10.1021/jp9941054
34. Chiu SW, Cheung YS, Ma NL, Li WK, Ng CY (1997) J Mol Struct Theochem 397:87. doi:10.1016/S0166-1280(96)05027-0
35. Lee HL, Li WK, Chiu SW (2003) J Mol Struct Theochem 629:237. doi:10.1016/S0166-1280(03)00146-5
36. Gomez B, Chattaraj PK, Chamorro E, Contreras R, Fuentealba P (2002) J Phys Chem A 106:11227. doi:10.1021/jp020437o
37. Lynch BJ, Truhlar DG (2002) J Phys Chem A 106:842. doi:10.1021/jp014002x
38. Lynch BJ, Truhlar DG (2001) J Phys Chem A 105:2936. doi:10.1021/jp004262z
39. Pu JZ, Truhlar DG (2005) J Phys Chem A 109:773. doi:10.1021/jp045574v
40. Zheng JJ, Zhao Y, Truhlar DG (2007) J Chem Theory Comput 3:569. doi:10.1021/ct600281g
41. Frisch MJ, Trucks GW, Schlegel HB, Scuseria GE, Robb MA, Cheeseman JR, Montgomery JA, Vreven T, Kudin KN, Burant JC, Millam JM, Iyengar SS, Tomasi J, Barone V, Mennucci B, Cossi M, Scalmani G, Rega N, Petersson GA, Nakatsuji H, Hada M, Ehara M, Toyota K, Fukuda R, Hasegawa J, Ishida M, Nakajima T, Honda Y, Kitao O, Nakai H, Klene M, Li X, Knox JE, Hratchian HP, Cross JB, Bakken V, Adamo C, Jaramillo J, Gomperts R, Stratmann RE, Yazyev O, Austin AJ, Cammi R, Pomelli C, Ochterski JW, Ayala PY, Morokuma K, Voth GA, Salvador P, Dannenberg JJ, Zakrzewski VG, Dapprich S, Daniels AD, Strain MC, Farkas O, Malick DK, Rabuck AD, Raghavachari K, Foresman JB, Ortiz JV, Cui Q, Baboul AG, Clifford S, Cioslowski J, Stefanov BB, Liu G, Liashenko A, Piskorz P, Komaromi I, Martin RL, Fox DJ, Keith T, Al-Laham MA, Peng CY, Nanayakkara A, Challacombe M, Gill PMW, Johnson B, Chen W, Wong MW, Gonzalez C, Pople JA (2004) Gaussian 03, revision B.03. Gaussian, Wallingford CT
42. Cramer CJ (2005) Essentials of computational chemistry: theories and models, 2nd edn. Wiley, Chichester
43. Baboul AG, Curtiss LA, Redfern PC, Raghavachari K (1999) J Chem Phys 110:7650. doi:10.1063/1.478676
44. Montgomery JA, Frisch MJ, Ochterski JW, Petersson GA (1999) J Chem Phys 110:2822. doi:10.1063/1.477924
45. Martin JML, de Oliveira G (1999) J Chem Phys 111:1843. doi:10.1063/1.479454
46. Truhlar DG (1998) Chem Phys Lett 294:45. doi:10.1016/S0009-2614(98)00866-5
47. Fast PL, Sanchez ML, Truhlar DG (1999) J Chem Phys 111:2921. doi:10.1063/1.479659
48. Schlegel HB (1986) J Chem Phys 84:4530. doi:10.1063/1.450026
49. Schlegel HB (1988) J Phys Chem 92:3075. doi:10.1021/j100322a014
50. Saeys M, Reyniers MF, Marin GB, Van Speybroeck V, Waroquier M (2003) J Phys Chem A 107:9147. doi:10.1021/jp021706d
51. Fernandez-Ramos A, Ellingson BA, Meana-Paneda R, Marques JMC, Truhlar DG (2007) Theor Chem Acc 118:813. doi:10.1007/s00214-007-0328-0
52. Scott AP, Radom L (1996) J Phys Chem 100:16502. doi:10.1021/jp960976r
53. Laidler KJ (1987) Chemical kinetics. Harper & Row, New York
54. Imai N, Dohmaru T, Toyama O (1965) Bull Chem Soc Jpn 38:639. doi:10.1246/bcsj.38.639
55. Eckart C (1930) Phys Rev 35:1303. doi:10.1103/PhysRev.35.1303
56. Vandeputte AG, Sabbe MK, Reyniers MF, Van Speybroeck V, Waroquier M, Marin GB (2007) J Phys Chem A 111:11771. doi:10.1021/jp075132u
57. Truong TN (2000) J Chem Phys 113:4957. doi:10.1063/1.1287839
58. NIST Computational Chemistry Comparison and Benchmark Database, Standard Reference Database 101, Release 12. (2005) http://srdata.nist.gov/cccbdb/
59. Altmann JA, Handy NC, Ingamells VE (1996) Int J Quantum Chem 57:533. doi:10.1002/(SICI)1097-461X(1996)57:4<533::AID-QUA1>3.0.CO;2-Z
60. Martin JML (1998) J Chem Phys 108:2791. doi:10.1063/1.475670
61. Durant JL (1996) Chem Phys Lett 256:595. doi:10.1016/0009-2614(96)00478-2
62. Dunning TH (1989) J Chem Phys 90:1007. doi:10.1063/1.456153
63. Woon DE, Dunning TH (1993) J Chem Phys 98:1358. doi:10.1063/1.464303

64. Martin JML, Uzan O (1998) Chem Phys Lett 282:16. doi: 10.1016/S0009-2614(97)01128-7
65. Dunning TH, Peterson KA, Wilson AK (2001) J Chem Phys 114:9244. doi:10.1063/1.1367373
66. Altmann JA, Handy NC, Ingamells VE (1997) Mol Phys 92:339. doi:10.1080/002689797170077
67. Altmann JA, Handy NC (1999) Phys Chem Chem Phys 1:5529. doi:10.1039/a907704i
68. NIST Chemistry webbook, Standard Reference Database 69, June 2005 Release. (2005) http://webbook.nist.gov/
69. Roy M, Mcmahon TB (1982) Org Mass Spectrom 17:392. doi: 10.1002/oms.1210170810
70. Jones A, Lossing FP (1967) J Phys Chem 71:4111. doi:10.1021/j100871a059
71. Ruscic B, Berkowitz J (1992) J Chem Phys 97:1818. doi:10.1063/1.463169
72. Hammerum S (1999) Chem Phys Lett 300:529. doi:10.1016/S0009-2614(98)01439-0
73. Ruscic B, Berkowitz J (1993) J Chem Phys 98:2568. doi:10.1063/1.464139
74. Kieninger M, Ventura ON (2002) Phys Chem Chem Phys 4:4328. doi:10.1039/b204643a
75. Benson SW (1968) Thermochemical kinetics, 1st edn. Wiley, New York
76. Van Speybroeck V, Van Neck D, Waroquier M, Wauters S, Saeys M, Marin GB (2000) J Phys Chem A 104:10939. doi:10.1021/jp002172o
77. Zhou C, Sendt K, Haynes BS (2008) J Phys Chem A 112:3239. doi:10.1021/jp710488d
78. Steudel R, Drozdova Y, Miaskiewicz K, Hertwig RH, Koch W (1997) J Am Chem Soc 119:1990. doi:10.1021/ja9624026
79. Migdisov AA, Suleimenov OM, Arekhin YV (1998) Geochim Cosmochim Acta 62:2627. doi:10.1016/S0016-7037(98)00188-4
80. Chemical Kinetics Database Standard Reference Database 17, Version 7.0 (Web Version), Release 1.3 (2005). http://kinetics.nist.gov/
81. Baker J, Muir M, Andzelm J (1995) J Chem Phys 102:2063. doi: 10.1063/1.468728
82. Sousa SF, Fernandes PA, Ramos MJ (2007) J Phys Chem A 111:10439. doi:10.1021/jp0734474
83. Patchkovskii S, Ziegler T (2002) J Chem Phys 116:7806. doi: 10.1063/1.1468640
84. Schipper PRT, Gritsenko OV, Baerends EJ (1999) J Chem Phys 111:4056. doi:10.1063/1.479707
85. Kurosaki Y, Takayanagi T (1999) J Chem Phys 111:10529. doi: 10.1063/1.480406
86. Zhang QZ, Sun TL, Zhou XH, Wang WX (2005) Chem Phys Lett 414:316. doi:10.1016/j.cplett.2005.08.084
87. Peng JP, Hu XH, Marshall P (1999) J Phys Chem A 103:5307. doi:10.1021/jp984242l
88. Karton A, Tarnopolsky A, Lamere JF, Schatz GC, Martin JML (2008) J Phys Chem A 112:12868. doi:10.1021/jp801805p
89. Baulch DL, Cobos CJ, Cox RA, Esser C, Frank P, Just T, Kerr JA, Pilling MJ, Troe J, Walker RW, Warnatz J (1992) J Phys Chem Ref Data 21:411
90. Voronkov MG, Kliuchnikov VA, Kolabin SN, Shvets GN, Varushin PI, Deriagina EN, Korchevin NA, Tsvetnitskaia SI (1989) Dokl Akad Nauk SSSR 307:1139
91. Frenkel M, Marsh KN, Wilhoit RC, Kabo GJ, Roganov GN (1994) Thermodynamics of organic compounds in the gas state. Thermodynamics Research Center, College Station
92. Chemical Kinetics Database NIST Standard Reference Database 17, (Web version), Release 1.4.2, Data version 08.09 (2008). http://kinetics.nist.gov/
93. Shum LGS, Benson SW (1985) Int J Chem Kinet 17:749. doi: 10.1002/kin.550170705